



Preparation and evaluation of graphene-based nanocomposite conductive hydrogels

Master of Engineering (Materials)

Nyi Nyi Tun

(Student No.: 2232585)

Supervisor: Professor Youhong Tang

Asst. Supervisor: Dr Wenjin Xing

Submitted to the College of Science and Engineering in partial fulfilment of the requirements for the degree of Master of Engineering (Materials) at Flinders University – Adelaide Australia

17/11/2021

Declaration

‘I certify that this thesis does not incorporate without acknowledgement any material previously submitted for a degree or diploma in any university; and that to the best of my knowledge and belief it does not contain any material previously published or written by another person except where due reference is made in the text.’

Nyi Nyi Tun

Date: 17/11/2021

ACKNOWLEDGEMENT

I would like to express my special thanks to my supervisor Professor Youhong Tang who goes above and beyond to make it right that this thesis was constantly on the correct path. His guidance and helpful feedback helped me make this project a success.

I would also like to express thanks to Dr. Wenjin Xing, my assistant supervisor. He was always there for me and provided his important support in fulfilling my experiments through this project.

I would like to show thanks to my family who is always being there for me.

Contents

| | |
|--|----|
| ACKNOWLEDGEMENT..... | 3 |
| List of tables..... | 6 |
| List of figures..... | 7 |
| Abstract..... | 9 |
| Chapter 1 Introduction..... | 9 |
| 1.1 Conductive hydrogels..... | 10 |
| 1.1.1 Carbon-based nanomaterials..... | 11 |
| 1.2 Biomedical applications of nanocomposite conductive hydrogels..... | 12 |
| 1.2.1 Biosensors..... | 12 |
| 1.2.2 Drug delivery..... | 13 |
| 1.2.3 Wound dressing..... | 13 |
| 1.2.4 Tissue regeneration..... | 13 |
| 1.3 Applications of stretchable strain sensors..... | 13 |
| 1.3.1 Healthcare and biomedical engineering..... | 14 |
| 1.3.2 Sport performance monitoring | 14 |
| 1.3.3 Interactive gaming and virtual reality | 15 |
| 1.3.4 Soft robotics and neuromechanics | 15 |
| 1.4 Problem statement | 16 |
| 1.5 Scope of the study..... | 16 |
| 1.6 Significant of research..... | 16 |
| 1.7 Objectives..... | 17 |
| Chapter 2 Literature review..... | 18 |
| 2.1 The importance of conductive hydrogels..... | 18 |
| 2.2 Nanocomposite hydrogels | 18 |
| 2.3 Nanocomposite conductive hydrogels | 20 |
| 2.3.1 Carbon nanotube conductive hydrogels..... | 20 |
| 2.3.2 Carbon fibre conductive hydrogels | 21 |
| 2.3.3 Carbon black conductive hydrogels | 21 |
| 2.3.4 Conductive hydrogels with graphene | 21 |

| | |
|--|----|
| 2.4 Properties of conductive hydrogels..... | 23 |
| 2.4.1 Mechanical properties | 23 |
| 2.4.2 Self-healing properties | 24 |
| 2.4.3 Biocompatibility..... | 25 |
| Chapter 3 Methodology..... | 26 |
| 3.1 Materials preparation..... | 26 |
| 3.1.1 Synthesis of PAM-GO hydrogel..... | 26 |
| 3.1.2 Synthesis of PAM-rGO hydrogel..... | 27 |
| 3.1.3 Synthesis of PAM-GO-rGO hydrogel..... | 29 |
| 3.2 Characterization..... | 30 |
| 3.2.1 Scanning electron microscopic (SEM) study..... | 30 |
| 3.2.2 Mechanical testing..... | 30 |
| 3.2.3 Conductivity measurements..... | 31 |
| 3.2.4 Sensitivity test..... | 32 |
| 3.2.5 Self-healing tests..... | 33 |
| 3.2.6 Adhesive properties of hydrogel..... | 33 |
| 3.2.7 Self-recovery test..... | 33 |
| Chapter 4 Result and discussion..... | 36 |
| 4.1 Characterization of nanocomposite hydrogels..... | 36 |
| 4.2 Mechanical properties | 37 |
| 4.3 Electrical measurements..... | 39 |
| 4.4 Self-recovery properties..... | 42 |
| 4.5 Self-healing properties..... | 45 |
| 4.6 Adhesive properties | 48 |
| Chapter 5 Conclusion..... | 51 |
| Chapter 6 Future work..... | 53 |
| References..... | 54 |

List of Tables

| | |
|--|----|
| Table 1: Ultimate tensile strength, elongation at break and young modulus for three nanocomposite hydrogels..... | 39 |
| Table 2: The values of electrical conductivity for three nanocomposite conductive hydrogels at different water content and gauge factor values to know sensitivity of these hydrogels for two liner regions..... | 42 |
| Table 3: The recovery rate of three nanocomposite hydrogels according to dissipated energy after 0.5 and 1 hour and the length changes percent after extending the samples to maximum length and releasing to normal state. | 44 |
| Table 4: Tensile strength values, elongation values at break and young modulus values before and after self-healing..... | 46 |
| Table 5: The recovery rate of tensile strength, strain and young modulus after self-healing... | 47 |
| Table 6: The electrical conductivity of three nanocomposite hydrogels before and after self-healing at different water content, the recovery rate of electrical conductivity after self-healing..... | 47 |
| Table 7: The various adhesive strength of three nanocomposite hydrogels on different substrates such as glass, steel and plastic..... | 48 |

List of Figures

| | |
|---|----|
| Figure 1: The fabrication of nanocomposite hydrogels using hydrogel and nanomaterial (Biondi, et al., 2015)..... | 11 |
| Figure 2: Applications of wearable strain sensors (Li Tang, et al., 2020) | 14 |
| Figure 3: The usage of nanocomposite hydrogels as wearable strain sensor on human skin (Souri, et al., 2020)..... | 19 |
| Figure 4: Nanocomposite conductive hydrogels from carbon-based nanomaterials such as carbon nanotubes and graphene (Biondi, et al., 2015)..... | 20 |
| Figure 5: The reduction of graphene oxide to reduced graphene oxide (Obodo, et al., 2019).. | 22 |
| Figure 6: The fabrication process of nanocomposite conductive hydrogels..... | 27 |
| Figure 7: The PAM-rGO solution A. before putting in the oven B. the nanocomposite hydrogels after taking from the oven..... | 29 |
| Figure 8: The samples preparation for the morphological observation under SEM..... | 30 |
| Figure 9: The load cell capacity with 500N for hydrogels..... | 31 |
| Figure 10: A. The Jandel RM 3000+ (four-point probe) machine for electrical testing, B. Agilent 34401A $6^{1/2}$ digital multimeter for electrical testing..... | 32 |
| Figure 11: SEM images of graphene-based hydrogels, A. SEM image of PAM-rGO at 20 μm , B. SEM image of PAM-GO-rGO at 40 μm , C. SEM image of PAM-GO at 200 μm | 37 |
| Figure 12: Stress-strain curves for mechanical behaviour of PAM-GO, PAM-rGO and PAM-GO-rGO hydrogels..... | 38 |
| Figure 13: Instron tensile testing system, A. the nanocomposite hydrogels before extension and B. the nanocomposite hydrogels while extension..... | 39 |
| Figure 14: The resistivity changes and strain curves for the sensitivity tests of three nanocomposite hydrogels..... | 41 |
| Figure 15: Testing and demonstration of electrical properties of three nanocomposite hydrogels, A. testing the electrical changes on different lengths of the samples, B. showing LED light brighter while using conductive hydrogels at normal length, C. showing the reduced brightness of LED light while using conductive hydrogels at extended length..... | 42 |

Figure 16: The extension of the samples into 7 times of original length and releasing nearly to its initial length, A. Before extension, B. while extension, C. after extension.....44

Figure 17: The structure of PAM with PDA and the formation of reversible bonds inside the hydrogels.....46

Figure 18: The stress-strain curves for the mechanical behaviour of three nanocomposite hydrogels after self-healing.....47

Figure 19: The interactions between free catechol groups which caused adhesion and the amino groups of PAM at green triangles and the reversible bonds formed between the catechol groups of the PDA chains.....49

Figure 20: The demonstration of the adhesive properties on different substrates including skin, glassware, steel and plastic.....50

Abstract

Owing to various unique properties, there have been a keen interest in the hydrogels to use in the biomedical field due to their rich water content, and biocompatibility. However, due to insufficient mechanical properties, low electrical conductivity, and short lifetime of conventional hydrogels, they were disrupted to use in large variety of applications. Thus, in this project, the conducting nanocomposite hydrogels were fabricated using mussel-inspired chemistry with a simple step procedure to improve various properties of conventional hydrogels, including mechanical and electrical properties by introducing graphene nanoparticles into polyacrylamide monomer (PAM). Remarkably, these hydrogels could be extended to 11 times of original length (higher than 1100%) and has tensile strength of 95 kPa and thus, these hydrogels integrate with high stretchability and strong mechanical strength. These hydrogels also showed high electrical conductivity of 0.0418 S/m at the water content of 89% and they demonstrated high sensing abilities by sensing small and large deformation. The self-healing properties of these hydrogels was received from their double-crosslinked polymer networks, which are physically and chemically crosslinked networks. The physically crosslinked networks helped to form the reversible self-treatment properties of hydrogels by interacting the ions between the ferric ions and carboxylic groups of acrylamide monomer and covalent bonds also helped to become stable and strong chemical network for these hydrogels. As graphene-based nanoparticles provided effective electric pathways, strain sensitivity can be achieved in these hydrogels and can detect the various deformation. In this project, the fabrication method is uncomplicated, simply scaled up, which will reduce the expense of preparation of hydrogels, and they can be used in wider applications including electronic skin and strain sensors due to higher electrical and mechanical properties.

Chapter 1. Introduction

In these days, wearable strain sensors have received tremendous attention in health monitoring, electronic skin, artificial intelligence, and soft robotics due to their unique properties such as flexibility, stretchability, self-recovery, self-healing, good adhesion and biocompatibility and these sensors also have the ability to convert the mechanical deformation into the electrical signal (Liu et al., 2020). Among various applications of these sensors, people are more interested in health monitoring and physiological monitoring as they would like to check and know their health condition and their body fitness every day. Thus, wearable strain sensors have been used by preparing with various sorts of materials including metals, semiconductors and polymers. Compared to these conventional devices fabricated by metals, semiconductors or rubbers, conductive hydrogels are the most popular ones due to their light weight, flexibility, and biocompatibility to produce wearable strain sensors (Tang et al., 2020). As the hydrogels are non-conductive polymers, conductive fillers including carbon-based nanomaterials are needed to add into them to become conductive hydrogels. By adding conductive nanofillers into non-conductive hydrogels, the important properties including mechanical and electrical properties were also increased in these hydrogels. Then, the properties of conductive hydrogels also depend on the water content in these hydrogels as hydrogels can absorb large amount of water in them (Yang, 2012).

1.1 Conductive hydrogels

To fabricate conductive hydrogels, ionic conductors, conducting polymers and conducting nanomaterials were used as the conductive fillers and they are added into the hydrogels. The conductive hydrogels with ionic conductors have some advantages such as low cost, easy preparation, and wide linear range. However, in these hydrogels, conductivity and sensitivity were still low level, and high salt concentration can also harm the cells. In the conductive hydrogels with conducting polymers, there are just few types of conductive polymers although the conductivity is high, and the dispersion is uniform in these conductive hydrogels. In the conductive hydrogels with conducting nanomaterials, they have high conductivity, sensitivity and steady contact interface although large extension will dislocate the conductive fillers and they are available only limited linear range. Depending on the composition of chemical elements, the conducting nanofillers can be separated into carbon-based, ceramic-based, polymeric-based and metal-based nanomaterials (Tang et al., 2020).

Image removed due to copyright restriction.

Figure 1: The fabrication of nanocomposite hydrogels using hydrogel and nanomaterial (Biondi et al., 2015)

1.1.1 Carbon-based nanomaterials

Carbon-based nanomaterials can be fabricated using carbon materials with the size ranging between 1 nm and 1 μm and carbon nanotubes (CNTs), carbon fibers (CFs), carbon black (CB) and graphene are the kinds of carbon nanomaterials. Among these carbon nanomaterials, CNTs and graphene have obtained more consideration in the application of biosensors, energy harvesting and drug delivery (Tang et al., 2020). CNTs and graphene were added into the traditional hydrogels to improved mechanical and electrical properties. CNTs are a kind of hydrophobic materials and can exist single-wall and multi-wall forms. The advantages of CNTs are excellent conductivity, high aspect ratio and outstanding stability in damp environments and due to these properties, they are highly used as the fillers to fabricate conductive hydrogels. However, CNTs have weak surface functional groups and they are hard to disperse and dissolve in the solvent. For this disadvantage, the surfaces of CNTs have been modified to use in fabricating conductive hydrogels, with organic molecular modification, amino

functionalization or carboxyl functionalization (Biondi et al., 2015). Graphene is thin and two-dimensional (2D) carbon-based nanomaterial which have one layer of carbon atom and it has the excellent conductivity in heat and electricity. Graphene has many superior properties such as electrical conductivity, great mechanical strength and molecular barrier abilities. However, the pure graphene has difficulties in bottom-up synthesis, agglomeration in solution and poor solubility. Thus, graphene can be changed as the hydrophilic materials by transformation into graphene oxide (GO) using some types of acid. In GO, it has the same hexagonal carbon structure to graphene and unlike graphene, GO also has hydroxyl, alkoxy, carbonyl, carboxylic acid and other oxygen-based functional groups. Compared with graphene, GO has improved in some properties such as higher solubility and surface functionalization which is important to use in nanocomposite materials (Smith et al., 2019). Due to high solubility of GO, it is easy to disperse in water and other solvents because of oxygen functionalities. This is an essential property to mix with other materials such as polymer or ceramic matrixes to improve their electrical and mechanical properties. However, GO has low conductivity and GO can be modified to fabricated reduced graphene oxide (rGO) using several methods by minimizing the number of oxygen groups and rGO has closer properties to those of pristine graphene. Compared with GO, rGO has higher electrical conductivity and mechanical properties and rGO become much more compliant for many applications. However, rGO is more difficult to dissolve in the solvents due to its possibility to create aggregates (Ray, 2015).

1.2 Biomedical applications of nanocomposite conductive hydrogels

Conductive hydrogels have received tremendous attention in several biomedical products due to their rare properties such as biocompatibility, conductivity, and flexibility. The most commonly used biomedical applications of nanocomposite conductive hydrogels are biosensors, drug supply, injury dressing and tissue regeneration (Xu et al., 2020).

1.2.1 Biosensors

Biosensors are assembled by integrating an electronic transducer and signing devices to measure the movement detection, biological recognition and electrophysiological signals. Compared with the traditional devices, conductive hydrogels put together the ability of high biocompatibility, easy fabrication, adjustable mechanical properties and responsive functionalities and it is beneficial to combine electronic devices with conductive hydrogels for the purpose of sensing. Thus, in the field of bioelectronics, conductive hydrogels are mostly

used as biosensors and these types of biosensors had enormous demands in health monitors, clinical diagnostics, and real-time biomolecule sensors (Xu et al., 2020).

1.2.2 Drug delivery

Many smart hydrogels have been produced as vehicles for the purposes of delivering drug using stimulus-responsive abilities which can react to light, ultrasound, and magnetic signals. For these hydrogels, another specific or large-size equipment is required to deliver drugs to the desire place. Compared to these devices with hydrogels, conductive hydrogels can produce electrical signals and with these signals, it is easier to use for drug delivery systems (Walker et al., 2019). Due to this easier feature, conductive hydrogels are ideal applications for precise and smart drug delivery devices. Thus, drug delivery systems combined with conductive hydrogels can release profiles to control the distance and dosage (Xu et al., 2020).

1.2.3 Wound dressing

The entire body of human is covered with skin and the skin can regulate physiological temperature and can also recognize exterior stimuli. Long-term wounds of human's skin can become a serious problem due to their high deadly condition to many possible health problems. Conductive materials including conductive hydrogels can be used to upregulate cellular activities of fibroblasts. Thus, several benefits have been found by using conductive hydrogels as wound dressing and these are to avoid infection of macrobacteria, to maintain moisture environment, to stop blood flow and to promote adhesiveness. For the purpose of designing wound dressing, the abilities such as biocompatibility, adhesiveness to tissue, low resistivity, antibacterial activity and haemostatic ability. Conductive hydrogels have all the features mentioned in the above to create wound dressings and synthetic skin and they also have easy preparation with multifunctionality (Xu et al., 2020).

1.2.4 Tissue regeneration

Conductive hydrogels were applied to imitate the extracellular matrix and transmit electrical signals to excitable cells including neural cells, muscular tissue cells and myocardial cells. Conductive hydrogels can also control the proliferation and isolation of these excitable cells using electrical stimulation. Moreover, conductive hydrogels already have a biocompatible environment, and they can offer a platform to deliver electrically excitable cells. However, it is still needed to focus on long term stability of conductive hydrogels including electrical, biological and mechanical properties. By combining exact microfabrication and appropriate

processability, conductive hydrogels can be designed as biomimetic constructs. Finally, to achieve the goal for tissue engineering, conductive hydrogels need more interdisciplinary association with cell-matrix format and in vivo performing (Xu et al., 2020).

1.3 Applications of stretchable strain sensors

Stretchable strain sensors are used in many applications in the range of detection of several human body changes such as heartbeat, respiration and body joints to human-machine dealings, virtual reality and interactive gaming.

Image removed due to copyright restriction.

Figure 2: Applications of wearable strain sensors (Tang et al., 2020)

1.3.1 Healthcare and biomedical engineering

Wearable strain sensors play in significant role in health sector, especially in healthcare monitoring devices due to their continuously detection of human body motion from large joint deformation to small movements including physiological signals such as respiration rates or pulse. For the purpose of monitoring the small strains, very responsive sensors are essential to achieve better outcome and precise signal changes in reaction to small deformations. By using wearable strain sensors, heart condition and respiration can be continuously monitored and can achieve important medical data for early access of different diseases such as heart failure, embolism, asthma and anemia (Souri et al., 2020).

1.3.2 Sport performance monitoring

Stretchable strain sensors can also be used to monitor sport performance by advancing another incorporated platform for measuring the biomedical and physiological factors of athletes. Wearable strain sensors can be applied on the various places of athletes' bodies and can be measured highly localized tracing of sport actions. Biophysical condition of athletes such as heart rates and respiration can be checked all the time using wearable strain sensors and can be achieved the information of deep insights of the physiological health condition of these players before, after and during the physical actions. Finally, strain sensors are the ideal applications to check continuously the health, fitness conditions, human-friendly treatment, and assessment of sportspersons' athletic performance (Souri et al., 2020).

1.3.3 Interactive gaming and virtual reality

Interesting one more usage of strain sensors are interactive gaming and virtual reality as these stretchable strain sensors can be used as the movement detectors for entertaining technology, including virtual reality. The figure illustrates the interactive gaming using wearable strain sensors as an example. Stretchable strain sensors using graphene were used on the fingers of hands and analysed their resistance variations while these fingers were bent and straightened, and these resistance changes can also be used as the commands to play a video game. For people who play video games for a long time, posture and body movement are also important while playing games and for that reasons, wearable strain sensors can be used as the devices in medical exercises, home-rehabilitation, and physical therapy. Moreover, stretchable strain sensors can be applied to cooperate with computer-generated environment or to monitor internet-of-things appliances and teleoperated programmed procedures (Souri et al., 2020).

1.3.4 Soft robotics and neuromechanics

In these days, roboticists and biologists are increasingly working together to analyse the mechanisms through soft robotic models with the abilities of more animal. These robotic models can be used as the tester for biologists to examine a higher experimentation with live animal and these tools will support in assumption analysing of motion dynamics, swimming actions, and how these animals make adaptable with complex environments such as sand, soils and land through the muscle and skeletal systems. For these purpose, wearable strain sensors are able to be used to achieve trustable sensory response that can produce strong abilities. In the modelling of animal motions during moving in a granular surface, stretchable strain sensors can be combined together with robot body that can give data about slip and inclination. The

usage of stretchable strain sensors can possibly extend in the field of biomechanics research to include diagnostics in veterinary care (Souri et al., 2020).

1.4 Problem statement

As mentioned in the previous sections, conductive hydrogels with various conductive fillers have both advantages and disadvantages to use in wide ranges of applications. Ionic conductive hydrogels have low conductivity, low sensitivity and high salt concentration, polymeric conductive hydrogels have only few types of conductive polymers and nanocomposite conductive hydrogels can cause fillers dislocation and can lose conductivity while large deformation. Nanocomposite conductive hydrogels are mostly used as the strain sensors in biomedical sector and due to their disadvantages, the applications of conductive hydrogels are restricted in biomedical area.

In this thesis, the primary interest is to expand the applications hydrogels and stay connected in these hydrogels during large deformation by using graphene-based material as the conductive fillers in the hydrogels and thus, these hydrogels can be applied in the broader range of biomedical usages. Due to their good conductivity in large deformation, potentially they can be used to sense large movements such as joints, knees, etc.

1.5 Scope of the study

In this thesis, the nanocomposite conductive hydrogels were prepared using graphene oxide, reduced graphene oxide and graphene oxide and reduced graphene oxide together as the conductive nanofillers. The various tests were performed on three conductive hydrogels samples and compared and analysed the differences between these samples. Finally, the significant properties of these samples will be discussed and make conclusion depending on their data or results.

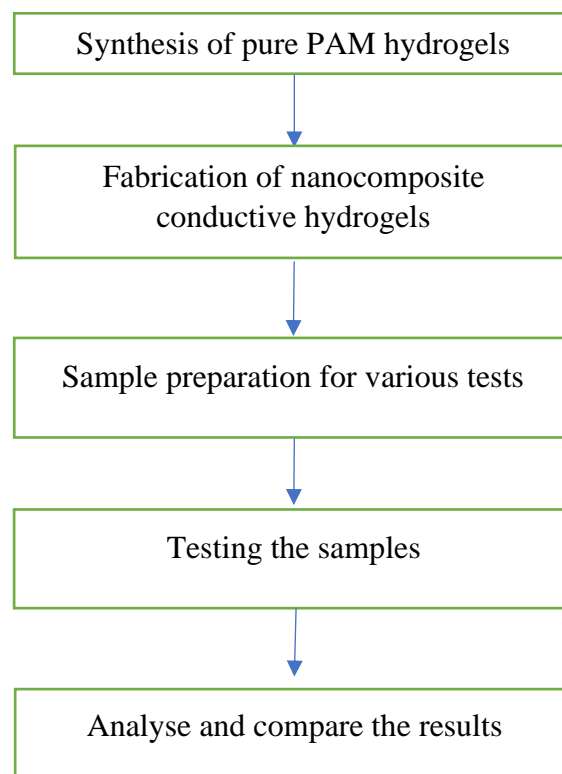
1.6 Significant of research

In this thesis, it is expected to have good electrical and mechanical properties of the composite conductive hydrogels over conventional hydrogel. The comparison can be achieved by performing the electrical and mechanical tests on conductive hydrogels and the properties of

hydrogels from literature. These hydrogels should have other properties such as good adhesion, self-recovery, self-healing and good sensitivity to use in most applications such as strain sensors. The main focus on this thesis is to evaluate the properties of various graphene-based nanocomposite hydrogels and to stay connected while extending the samples into large deformation.

1.7 Objectives

The first aim of this thesis is to prepare nanocomposite conductive hydrogels by introducing graphene oxide and reduced graphene oxide into the hydrogels. By adding conductive nanofillers into the hydrogels, it will increase electrical and mechanical properties of the hydrogels and it will also affect other properties of the hydrogels. After fabricating nanocomposite conductive hydrogels, another objective is to investigate the properties of these hydrogels such as mechanical properties, electrical properties, adhesive properties, self-recovery and self-healing. Then, the results from these samples will be compared each other depending on their high-water content. The resistivity changes will be recorded by extending the conductive hydrogels samples from 20% extension as the small deformation to 200% extension as the large deformation. Finally, the significant data from the various properties will be reviewed and make sure that these hydrogels can be applied in various applications such as strain sensors.





Demonstration for electrical
conductivity changes using LED

Chapter 2. Literature review

In this thesis, nanocomposite hydrogels were fabricated to expand the conductive properties and mechanical properties of hydrogels and to enhance the usage of hydrogels in the biomedical area. In literature review section, the importance of conductive nanocomposite hydrogels will be discussed along various properties of hydrogels and other previous works on hydrogels. The properties of nanocomposite hydrogels will be analysed by performing various tests and compare the results against previous works.

2.1 The importance of conductive hydrogels

Hydrogel is a kind of soft materials and is popular in these days due to its unique properties and wide applications in medical fields. However, pure hydrogels, including pure PAM hydrogels, do not exhibit high electrical conductivity, high stretchability, high mechanical properties and thus, these pure hydrogels can be used in small number of applications although these hydrogels have great prospects to be applied in most applications. Therefore, pure hydrogels are needed to be modified by adding some chemical materials to improve its important properties to use in most application. Nowadays, hydrogels are widely used in most medical sensors for various purposes and in sensors, high conductivity is very important to achieve the data exactly and quickly. Thus, nanocomposite hydrogels are well known for high conductivity and high mechanical properties.

2.2 Nanocomposite hydrogels

Hydrogels have a three-dimensional (3D) polymer network and are popular due to their ability to hold large volume of water within their polymer network, which can be used in most engineering applications. However, there were some limitations in the applications of hydrogels fabricated traditionally by physically or chemically crosslinking. In physically cross-linked gels, the physical interaction such as hydrogen bonding, $\pi - \pi$ interaction and electrostatic interaction are not strong enough and reversible and as a result, they have low mechanical properties. Then, in facing some physical situations, including temperature, pH and ionic strength changes, the produced hydrogels are easy to loosen and broken. In chemically cross-linked gels, due to rigid and permanent covalent bonds, they have higher mechanical properties. However, as the networks of these gels are formed with the arrangement of irregular

chemical crosslinkers and the polymer chains' lengths are not long enough at the cross-linked points, the mechanical stress such as bending, stretching and compression cannot be resisted in these hydrogels. Nanocomposite hydrogels are three-dimensional networks with hybrid structures, and they are manufactured with nanomaterials and physically or chemically cross-linked polymer chains. When the nanomaterials are mixed with the networks of polymer hydrogels, the hydrophilic chains of polymer can greatly combine with the huge surfaces of nanomaterials, and this can cause nanocomposite hydrogels to have high toughness and strength. Moreover, nanomaterials' large surfaces have the ability to support more protein absorption and focal adhesion sites, which can adhere cells. Thus, combination nanomaterials with hydrogels can increase the adhesiveness of protein and cell on nanocomposite hydrogels. Furthermore, by using carbon-based or metal-based nanomaterials, nanocomposite hydrogels show unique characteristics, including magnetic or electricity conductivity for the purpose of wider applications (Zhao et al., 2020).

Although there are small numbers of applications with pure hydrogels as mentioned in the above, improvements have been found in the biomedical applications after adding conductive nanofillers into the hydrogels. For example, CS/Ag-NPs and CNFs/alginate/Ag-NPs nanocomposite hydrogels were used for disinfectant products, CMC/gelatin/Ag-NPs and CS/gelatin/Ag-NPs nanocomposite hydrogels for wound healing, CS/Ag-NPs and CS/PVA/Ag-NPs for biomedical applications, PVA/GO/Ag-NPs nanocomposite conductive hydrogel for injury dressing and antibacterial and PAM/CMC/Ag-NPs nanocomposite conductive hydrogels for drug delivery respectively in the biomedical sectors (Wahid et al., 2020).

Image removed due to copyright restriction.

Figure 3: The usage of nanocomposite hydrogels as wearable strain sensor on human skin (Souri et al., 2020)

2.3 Nanocomposite conductive hydrogels

Although various kinds of nanomaterials including carbon-based nanomaterials, and metal-based nanomaterials are able to be used to fabricate nanocomposite hydrogels, carbon-based nanomaterials are most suitable and popular materials to fabricate nanocomposite conductive hydrogels due to easy preparation, higher conductivity and fewer drawbacks.

Image removed due to copyright restriction.

Figure 4: Nanocomposite conductive hydrogels from carbon-based nanomaterials such as carbon nanotubes and graphene (Biondi et al., 2015)

2.3.1 Carbon nanotube conductive hydrogels

Carbon nanotubes (CNTs) are one of the most popular nanomaterials to fabricate nanocomposite materials due to their novel qualities including high mechanical properties, low mass density, high-level specific area and superior thermal and electrical conduction. Mostly, CNTs are applied on hydrogels to enhance the mechanical properties of these conductive hydrogels as the reinforcing agents. By combining CNTs and hydrogels together, very tough and higher electrically conductive hydrogels are obtained. Moreover, CNTs based

nanocomposite hydrogels have adaptable platform for improving hydrogels with several responsive properties and outstanding mechanical performance. However, there is a problem in using CNTs in hydrogels due to the toxic effects of CNTs, and these effects can damage the biocompatibility of hydrogels and these effects can be reduced by functionalizing and incorporating CNTs in hydrogel's networks (Mihajlovic et al., 2019). Thus, CNTs based hybrid hydrogels are applied in a variety of applications including medical applications such as tissue engineering, implantable devices, regenerative medicine, bio-sensing, bio-robotics and drug delivery devices (Vashist et al., 2018).

2.3.2 Carbon fibre conductive hydrogels

Carbon fibres (CF) are also one of the most popular materials to produce nanocomposite hydrogels for the purpose of various applications, especially in energy storage and drug delivery and they have unique abilities such as high structural stability, environmental friendlies, superior electrical conductivity, light weight and low cost. However, pristine carbon fibres have extremely low surface area and thus, these materials display very poor electrochemical performance. For this reason, these materials can be merged with high-surface-area carbon-based nanomaterials to deliver superior electrical dual layer capacitance (Li et al., 2019). By adding CF into the hydrogels, it increases greatly in the mechanical properties and the thinner CFs can increase the mechanical properties of composite hydrogels than thicker ones. In the drug delivery systems, the accumulative quantity of release and releasing time depend on the pore volume and the surface area of CFs. Using CFs in hydrogels can increase the drug release about four times longer and mechanical properties about 2.6 times higher as CFs can act as the drug reinforcement and reservoir and these CFs-containing hydrogels also have biocompatible behaviour (Yun et al., 2011).

2.3.3 Carbon black conductive hydrogels

Although carbon black (CB) has excellent properties such as electrical conductivity, heat resistance, chemical stability and safe features, dispersity and stability of carbon black are very poor in aqueous solution. Due to their low hydrophilicity, there is a potential to become aggregate in carbon black particles and thus, modification of these particles is a great important to use in hydrogel preparation. Various modification methods of carbon black such as surface coating, oxidation modification, oxidation modification and dispersion modification, were developed to surface alteration and functionalization of CB (Zhu, et a., 2012). After incorporating carbon black nanoparticles (CNPs) into hydrogels during gelation, CNPs have

the ability with the higher molecular loading ability. Then, these CNPs are able to be fabricated to come up with uniform size and they are also biocompatible. Due to the surface properties and high porosity of CNTs, the hydrogels with CNTs are very popular to interact with antibiotic medicine such as vancomycin for drug delivery and hydrogels with CNPs can also increase the timescale and amount for drug release (Shukla et al., 2018).

2.3.4 Conductive hydrogels with graphene

Graphene is a kind of carbon material with 2-dimensional atomic thickness and shows higher mechanical and electrical properties. From graphene, graphene oxide (GO) can be fabricated by harsh oxidation process from the oxidative exfoliation of graphite. However, in GO, it displays weak electrical properties as a result of the flaws in its structure. Thus, GO is able to be degraded to become reduced graphene oxide (rGO) with conductivity by partially replacing carbon bonds. Nevertheless, reduced graphene oxide displays poor solubility in aqueous media. GO and rGO was highly used as the parts of biomaterials as they can encourage the interaction between molecular and cellular structures. Graphene-based conductive hydrogels provide advanced properties including stability in electrical and mechanical abilities as graphene derivatives can greatly cooperate with polymer networks and do not need any dopants for their conductivity (Jo et al., 2017). Graphene based hydrogels can be produced by adding either polymers, macromolecules, cations, or small organic molecules into aqueous dispersion of graphene derivatives. The fabrication of graphene based various hybrid systems have got tremendous consideration in nanomaterial study because of their usages in various areas such as biomedical fields, fuel cells, catalysts, energy conversion and others (Adhikari et al., 2012). Therefore, Yang et al., fabricated the smart hydrogels by introducing reduced graphene oxide and showed excellent electro-response and improved mechanical properties to use as the soft actuators. RGO nanosheets were introduced into poly(2-acrylamideo-2-methylpropanesulfonic acid-co-acrylamide) (poly(AMPS-co-AAM)) hydrogel to get the excellent electro-response and mechanical properties in their reports. Due to good conductivity of rGO nanosheets, rGO-based poly(AMPS-co-AAM) hydrogels showed an immediate and considerable response to an electrical stimulus as higher conductivity can increase the ion transport in the polymer network. Then, by adding rGO nanosheets, the composite structure between polymer matrix and rGO nanosheets was beneficial for dissipating energy and thus, the tensile and compressive strength were also improved in these hydrogels (Yang, et al., 2017).

Image removed due to copyright restriction.

Figure 5: The reduction of graphene oxide to reduced graphene oxide (Obodo et al., 2019)

2.4 Properties of conductive hydrogels

Conductive hydrogels are widely used in many applications including wearable or implantable electronics and bioelectronics in these days as a result of their unique abilities such as mechanical properties, electrical abilities, self-healing properties and biocompatibility. By adding with nanomaterials, tuneable and great properties of conductive hydrogels can be achieved, and they can be expected to enrich their applications in many fields (Guo et al., 2019).

2.4.1 Mechanical properties

Poor stretchability and brittleness can greatly prohibit to use in various applications for the traditional polymer materials. Compared to these polymer materials, conductive polymer hydrogels have the outstanding properties with tuneable mechanical properties, and they can be fabricated to enhance the mechanical properties with great efforts. Porosity is one of the great features in conductive polymer hydrogels, that can increase the mechanical abilities of conductive polymer hydrogels in various methods such as free volume content, connectivity, size, and surface properties. Fabricating cavity nanospheres of conductive polymer hydrogels is a good way to improve mechanical properties as porous nanostructures of these hydrogels have the ability to withstand larger deformation while bending. Network of conductive polymer hydrogels can be joined randomly to provide highly structural elasticity. Moreover, crosslinked double network is the best way to deal with weak mechanical abilities of conductive polymer

hydrogels by achieving reversible crosslinking such as ionic bonding, hydrogen bonding or lamellar bilayer. In double network, two polymers are interconnected with different physical properties and first network is rigid framework and second network is ductile substance. Because of the innate structural dissimilarity and the absence of proper energy dissipation mechanism, the poor mechanical properties have been found in conductive polymer hydrogels. The crosslinked double network can help conductive polymer hydrogels for mechanical enhancement, that depends on the sacrificial bond of rigid framework which encourages the energy dissipation by shielding ductile substance which sustains stress through huge expansion. The hydrogels with double crosslinked single network can provide hydrogel with excellent strength and stretchability when compared to double network hydrogels. Higher swelling capacity and adjustable superior mechanical properties are generally not accessible simultaneously in most covalently crosslinked hydrogels (Guo et al., 2019). For this problem, Zhong et al. fabricated polyacrylic acid (PAA) hydrogels with dual crosslinked single network and ionic and covalent crosslinking were used in these hydrogels to deplete energy and provide the original structure of the network. These hydrogels show superior mechanical properties by enabling its original condition after bending, knotting, compressing, and high stretching (Zhong et al., 2016).

Without using previous strategy, a simple soaking method can also be applied to increase mechanical capacities of the conductive polymer hydrogels. By applying soaking method, Yang et al. converted conductive hydrogels into really hard dual network hydrogels. To synthesis composite hydrogels, free-radical polymerisation of acrylamide (AM) and Chitosan was immersed in both NaOH and NaCl solution to produce double network hydrogel and Chitosan physical network formed by soaking and covalent poly-acrylamide chains made to form double network hydrogels. In this innovative physical chains, greater crosslink density and reduced size of pore are the major reason for increasing toughness of hydrogel (Yang et al., 2016). Thus, a wide variety of methods can be used to improve the mechanical abilities of conductive polymer hydrogels and due to superior mechanical properties, these hydrogels can be applied in wide range of products and fields.

2.4.2 Self-healing properties

Self-healing is an essential abilities of conductive polymer hydrogels and biological bone and skin also have the same self-healing property. Using this self-healing property in all types of electronic devices, the function and structure of the product can be restored after damaging the

product and thus, it can increase the life of the device and reduce the costs of maintenance. In two types of self-healing, external interventions are not required in automatic self-healing although nonautomatic self-healing required additional internal stimuli. Dynamic covalent chemistry is one of the useful ways to fabricate inherently self-treatment conductive polymer hydrogels (Guo et al., 2019). Liu et al. fabricated single network hydrogel with a novel dynamic-covalent bond using two component gelator: calix[4]pyrrole-derivative (CPTH) and poly (ethylene glycol) (PEG-DA). These hydrogels showed good mechanical properties and excellent self-treatment abilities due to reversibility of the dynamic nature of the acylhydrazone bond (Liu et al., 2018). Noncovalent interactions can also be used to achieve autonomous self-healing such as ionic bond, host-guest interaction, hydrophobic bonding, and hydrogen bonding. Chen et al. fabricated self-healing and self-recovery hydrogel by crosslinking numerous hydrogen bonding groups into PANi/PSS network. Hydrogen bonds' dynamic reversibility helped to reconstruct the network and dissipate energy, and these are essential self-healing properties of hydrogels. Using this method, the hydrogel can be restored by contacting 30s after cutting into two pieces and can also withstand stretching (Chen et al., 2019).

2.4.3 Biocompatibility

Wearable or implantable are needed to make connection directly with human skin and they are essential to provide safety to human health. With excellent hydrated environment and tuneable physicochemical properties, conductive polymer hydrogels are regarded a good applicant of biocompatible material and have been extensively applied in a lot of biological gadgets including biosensor, cell culture, drug delivery and tissue engineering. As organic compositions have similar structures with extracellular matrix of biological tissues, conductive polymer hydrogels have been used in bioelectronic interfaces as the next generation of biology and electronics. Then, conductive polymer hydrogels also show excellent mechanical properties, good conductivity and water-rich nature, which match for biomechanical properties to use as tissue-electrode interfaces (Guo et al., 2019). Li et al. prepared biocompatible polypyrrole hydrogel to use as the repairer for spinal cord damage by using tannic acid as the crosslinker and dopant. Moreover, synthetic electrical organs can be produced using the packed PAM hydrogels, and these organs show biocompatibility and flexibility contrasted to traditional batteries and demonstrate its wonderful ability in operating implants (Zhou et al., 2018). Combining conductive polymer hydrogels with natural polymer materials have received tremendous attention for biopolymeric biomaterial applications. From the syntheses of biocompatible conductive polymer hydrogels, gelatin, chitin and alginate have been achieved

as a biodegradable and biocompatible functional material and it was shown that ordinary polymers can improve adhesion of cell and build physical crosslinks to increase the mechanical abilities of conductive polymer hydrogels. Gan et al. developed a biocompatible hydrogel using polypyrrole, chitosan and polyacrylamide and in this composite hydrogel, good properties were shown in wound healing, cell adhesion and drug delivery. This hydrogel can also heal the wound faster and have better tissue integrity than the control group (Gan et al., 2018).

Chapter 3. Methodology

3.1 Material preparation

After the literature papers have been reviewed, the various kinds of hydrogels were synthesized as the next step. The first aim of my thesis is to fabricate nanocomposite conductive hydrogels using conductive nanofillers such as graphene oxide and reduced graphene oxide. Acrylamide monomer (AM), dopamine (DA), ammonium persulfate (APS), N, N'-methylenebisacrylamide (MBA) and N, N, N', N'-tetramethylethylenediamine (TEMED) were purchased from Sigma-Aldrich and these are used without doing any modifications. Graphene oxide and reduced graphene oxide were purchased from ACS Material and milli-Q water, LABEC mrc and IKA Vortex 3 shaker were available in Advanced Materials Laboratory of Flinders University.

Before fabricating nanocomposite conductive hydrogels, the conventional hydrogel was firstly prepared with one step polymerisation by following the method done by Yu et al. (2015). To prepare PAM hydrogel, APS was used as an initiator to start the process of polymerization and MBA was used as a crosslinker in the solution to improve the bonding between polymeric chains. TEMED was used as a catalyst to be faster the process of chemical reaction. Firstly, 1.25 g of AM was combined with 10mL of Milli-Q water at the ambient temperature and stirred for 15 minutes under magnetic stirring to fully neutralize the AM monomer. After that, 7.27 mg of APS was added as the thermal initiator, and 2 mg of MBA was put into the AM solution. Then, the acquired mixture was applied by vigorous shaking using an IKA Vortex 3 shaker (Sigma-Aldrich, Sydney, Australia) to have better homogeneity. The final solution was added into a glass dish with the diameter of about 90mm and put the dish into an oven to heat under the temperature of 60°C for 2 hours. After 2 hours, the dish was taken from the oven and the synthesised PAM hydrogels were taken from the glass dish and put in closed plastic bags in the fridge and waited for two days to test the samples.

3.1.1 Synthesis of PAM-GO hydrogel

After fabricating PAM hydrogels successfully, PAM-GO hydrogels were synthesised based on the previous PAM hydrogels preparation and by following Tai et al. (2013). To prepare PAM-GO hydrogel samples, firstly 3.13 ml of graphene oxide was combined with 10ml of milli-Q water and stirred with hand for a while to be homogenous. Then, graphene oxide solution was sonicated by a LABEC mrc sonic-950 wt at 950 w for 2 minutes. On the other hand, polydopamine (PDA) was prepared by dissolving DA (0.0625g) into NaOH (5.75 mL) and

APS (0.25) was added into the solution by stirring for 2h. Then, 1.25 g of AM and PDA solution were put into the graphene oxide solution. The GO-AM mixture was stirred under the magnetic stirrer for 5 minutes and the mixture was completely mixed using the IKA Vortex 3 shaker for 5 minutes. It is essential to be homogenous in the solution when preparing PAM-GO hydrogels. Subsequently, 0.00725 g of APS, 0.002 g of MBA and 0.0125 g of FeCl₃ are added as the thermal initiator and cross-linker into the AM-GO solution and followed by vigorous shaking for 5 minutes. On the other hand, 1 ml of TEMED was taken and mixed with 50 ml of milli-Q water and 0.2 ml of TEMED solution was put into the AM-GO solution and used as the catalyst to speed up the process of the polymerization. To make sure the homogeneity of the solution, the solution was processed under the vigorous shaking again for 5 minutes. Finally, the final solution was transferred into the dish of 90 mm diameter and put the dish in the oven at the temperature of 60°C for 12 hours. After 12 hours in the oven, PAM-GO hydrogel was washed with water for three times and peeled off from the oven and placed the hydrogel in the sealed in the fridge and waited for two days to test.

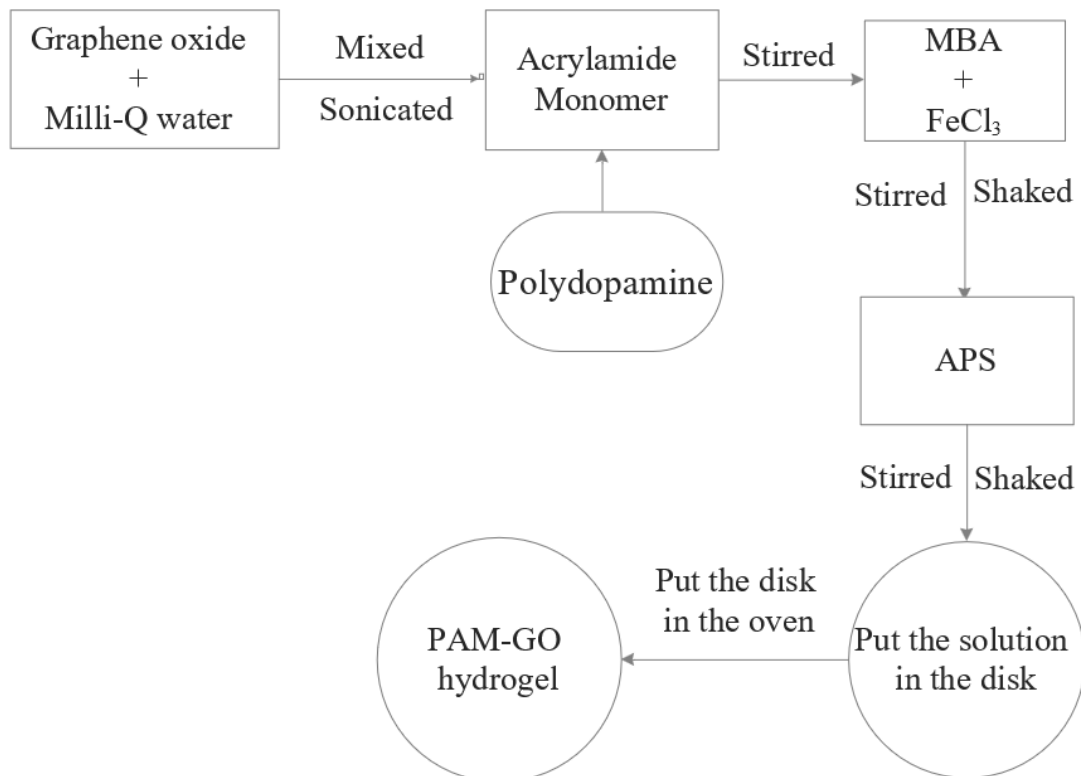


Figure 6: The fabrication process of nanocomposite conductive hydrogels

3.1.2 Synthesis of PAM-rGO hydrogel

Unlike with graphene oxide, rGO is a kind of hydrophobic material, and it shows low dispersibility in aqueous. For preparation of PAM-rGO, it took more time and was more difficult to be homogenous in the solution when compared with PAM-GO hydrogel preparation. Firstly, PAM-rGO hydrogel was prepared using the same preparation method with PAM-GO hydrogel preparation by substituting rGO instead of GO. However, due to low solubility of rGO, rGO nanoparticles were not fully homogenous in the PAM solution. Thus, various solvents such as ethanol and N-methyl-2-pyrrolidone (NMP) were used to improve the solubility of rGO. According to Ma et al. and Johnson et al., NMP solvent can increase the solubility rate with 9.4 rGO solubility/ $\mu\text{g}\cdot\text{ml}^{-1}$ and ethanol can increase the solubility rate with 0.91 rGO solubility/ $\mu\text{g}\cdot\text{ml}^{-1}$ (Ma et al., 2018) (Johnson et al., 2015). Therefore, ethanol and NMP solvents were combined with rGO and sonicated for 2 minutes, and it was found that the solubility of rGO was so much better. However, unlike water, these high solubility solvents are difficult to evaporate and disturbed the polymerization of hydrogel even adding small amount of these solvents. Hence, milli-Q water was used to prepare PAM-rGO hydrogel and stirred more hours than PAM-GO preparation method. To prepare PAM-rGO hydrogel samples, firstly 0.01 g of reduced graphene oxide was combined with 10 ml of milli-Q water and stirred with hand for 5 minutes to be homogenous. Then, graphene oxide solution was sonicated by a LABEC mrc sonic-950 wt at 950 w for 4 minutes and 1.25 g of AM and PDA were added into the reduced graphene oxide solution. The rGO-AM mixture was stirred under the magnetic stirrer for 15 minutes and the solution was completely mixed using the IKA Vortex 3 shaker for 5 minutes. Subsequently, 0.002 g of MBA and 0.0125 g of FeCl_3^+ were added into the rGO-AM solution and stirred for 1 hour under magnetic stirring, followed by vigorous shaking for 5 minutes. Then, 0.00725 g of APS was put into the solution and stirred another 1 hour under magnetic stirring to be fully homogenous. After that, the rest steps are the same with PAM-GO sample preparation and when PAM-rGO hydrogel had been successfully fabricated, the sample was washed and put in the fridge for two days to test.

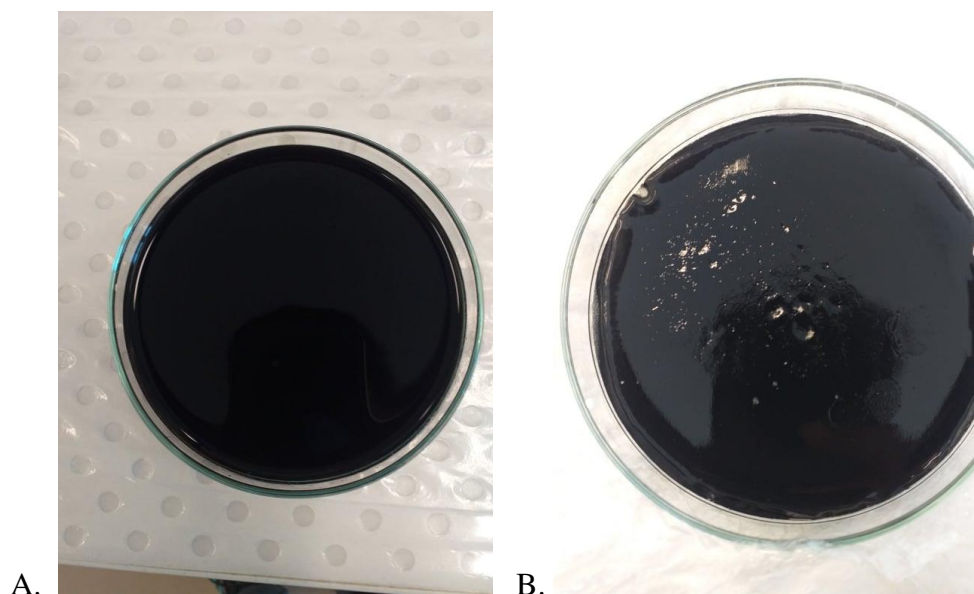


Figure 7: The PAM-rGO solution A. before putting in the oven B. the nanocomposite hydrogels after taking from the oven

3.1.3 Synthesis of PAM-GO-rGO hydrogel

The preparation of PAM-GO-rGO hydrogel was nearly the same fabrication method with PAM-GO hydrogel and PAM-rGO hydrogel preparation. However, the stirring times under magnetic stirrer were different due to different solubility properties of graphene nanoparticles. When the stirring times were set about 15 minutes, GO and rGO solution were not fully dispersed in the AM solution and when the stirring times were set about 1 hour, GO and rGO nanoparticles became flakes in the AM solution without being homogenous. Thus, about 30 minutes stirring times were used to be homogenous for the preparation of PAM-GO-rGO hydrogel. Firstly, 1.6 ml of GO and 0.005 g of rGO were mixed together and stirred with hand for a while and mixed with 5 ml of milli-Q water. Then, the GO-rGO solution was sonicated for 2 minutes and centrifuged for 5 minutes in the centrifuge machine to know the homogeneity of the solution. On the other hand, 5 ml of milli-Q water, 1.25 g of AM and PDA were mixed and stirred for 15 minutes under magnetic stirrer. Next, GO-rGO solution and AM solution were mixed and stirred for 30 minutes, followed by vigorous shaking for 5 minutes. Subsequently, 0.00725 g of APS, 0.002 g of MBA and 0.0125 g of FeCl_3 were put into the solution and stirred for 30 minutes again. After that, the rest steps are the same with PAM-GO sample preparation and when PAM-GO-rGO hydrogel had been successfully fabricated, the sample was washed and put in the fridge for two days to test.

3.2 Characterization

After successfully fabricating the nanocomposite conductive hydrogels, the various tests are needed to be done to know their actual properties inside them and compared the properties each other. In the characterization of these hydrogel samples, mechanical properties, electrical properties, self-healing properties, self-recovery, adhesion properties and sensitivity were tested depending on their water content. To get the accurate properties of the samples, about three tests were performed to measure each property and different samples were prepared for different properties.

3.2.1 Scanning electron microscopic (SEM) study

To observe the morphology of nanocomposite hydrogels, scanning electron microscopy (SEM) (EDAX SEM) was employed. Firstly, the hydrogel samples were freeze-dried in the oven for 6 hours at 60°C as the moisture from the sample can damage the SEM machine. Then, each hydrogel sample was put in different pin stubs as show in figure and the samples and pin stubs were taped together by using carbon double tape. After that, the samples were coated with platinum about 0.5 mm thickness to get a conductive environment and the samples were put in the SEM machine. Finally, various SEM images were taken by using various spatial resolution starting from 20 μm to 500 μm in different places of the samples.



Figure 8: The samples preparation for the morphological observation under SEM

3.2.2 Mechanical testing

To check the mechanical properties of prepared nanocomposite conductive hydrogels, uniaxial tensile was performed with universal testing equipment (Instron 5960, Norwood, MA, USA) at the room temperature using a load-cell capacity of 500N. The speed of the crosshead was set as 10 mm/min for all hydrogel samples. In the tensile test, the samples were put between two clamps in the machine and the tensile force was used into the sample by pulling apart. To get the data from the test, the testing system automatically recorded the displacement (mm) and load values (N) for the samples. The shapes of the prepared samples were rectangular shape by cutting with a razor and the lengths between the rigid clamps and width of the samples kept about 10 mm and 20 mm respectively. The thickness of the samples was about 1.1-1.5 mm, and all the dimensions were measured using a digital vernier caliper for each sample. The nominal stress σ was calculated using the following equation.

$$\sigma = \frac{F}{A}$$

F = Tensile force or applied load, A = Cross sectional area

The strain was also evaluated using the following equation.

$$\text{Strain} = \frac{\Delta L}{L} = \frac{L-L_0}{L_0}$$

ΔL = Change in length, L_0 = Original length, L = Current length



Figure 9: The load cell capacity with 500N for hydrogels

3.2.3 Conductivity measurements

In conductivity measurement, the samples were cut as the rectangular shapes using by a razor and its dimensions were 48 mm in length, 16 mm in width and 2.2 mm in height. Firstly, the cut hydrogel sample was tested using digital multimeter (two points) and in using digital multimeter, the two digital cable wire pens were put on each edge of the sample for three or four times and record the resistance of the sample. To get more accurate data, four-point probe method was used for each sample using Jandel RM 3000+ (four points) machine. Based on the resistance of the sample, the resistivity of the sample was calculated using the following the equations.

$$\rho = R \frac{A}{L}$$

ρ = Resistivity of the sample

R = Resistance of the sample

A = Cross sectional area of the sample

L = Length of the sample

Then, conductivity of the sample was determined using $\sigma = \frac{1}{\rho}$. After that, the hydrogel sample was connected to a circuit with LED by applying different amount of voltage using a Keithley 2500 source meter and checked the input voltage and output voltage of the circuit. Finally, the different resistance values of the sample were calculated and recorded by stretching the hydrogel sample and depending on the different length of the sample.

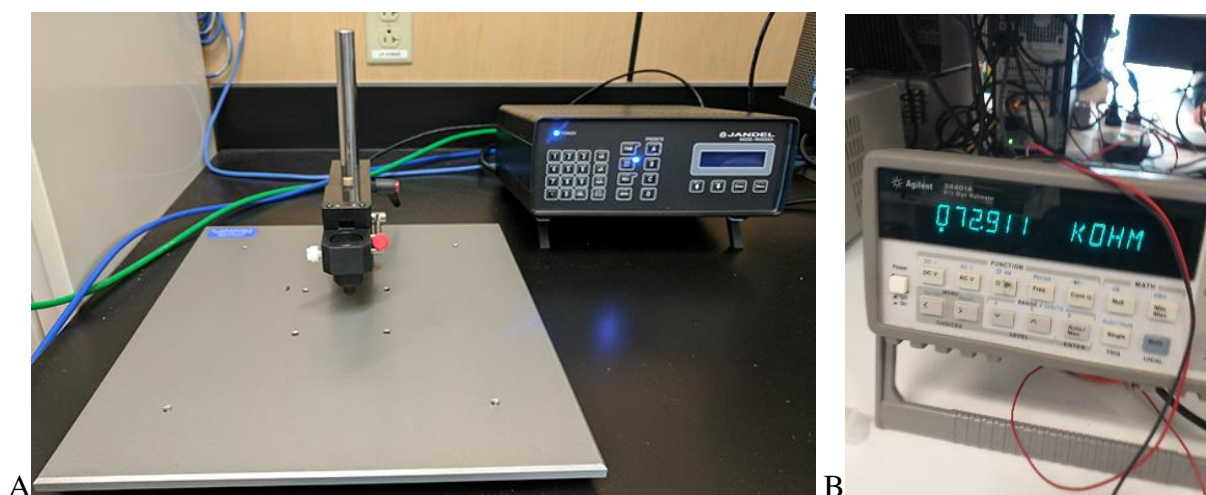


Figure 10: A. The Jandel RM 3000+ (four-point probe) machine for electrical testing, B. Agilent 34401A 6¹/₂ digit digital multimeter for electrical testing

3.2.4 Sensitivity test

For sensitivity test of the samples, the samples were also the rectangular shapes cut by razor and the same dimensions was used from the conductivity measurement with 48 mm in length, 16 mm in width and 2.2 mm in height. For the purpose of sensing performance tests, the resistivity changes have been calculated depending on the strain of the samples by using four-point probe measurement with Jandel RM 3000+ (four points). For strain of the samples, the samples were extended from 20% to 200% by using hand and taped two ends of the samples on the ruler as shown in figure. From the resistivity changes and the length changes, the gauge factor (G.F) was calculated for the strain sensor using the following equation.

$$G.F = \frac{\Delta R/R_0}{\Delta L/L_0} = \frac{(R-R_0)/R_0}{(L-L_0)/L_0}$$

R, R₀ = The resistance of the original and stretched hydrogels

L, L₀ = The length of the original and stretched hydrogels

3.2.5 Self-healing tests

For self-healing test, the hydrogel samples were cut into two pieces by using razor and the parts of the cut hydrogels were contacted again and taped in the cut area as shown figure. Then, the samples were sealed using the storage bags and put in the fridge for 2 days. After 2 days, the samples were prepared to test mechanical properties under Instron tensile machine and electrical properties using Jandel RM 3000+ and compared their results before and after self-healing test.

3.2.6 Adhesive properties of hydrogel

Adhesion tests were accomplished to calculate the adhesive properties of the nanocomposite conductive hydrogels using various substrates such as metal, glass and polymer. For sample preparation, the hydrogel samples were attached to the polished iron surface on one side and the tested substrates such as iron, glass and polymer were attached on another side of the hydrogels. Then, the force was used on the prepared hydrogels to separate the two substrates and the adhesion strength of the hydrogel (σ) was evaluated using the following equation.

$$\sigma = F_{\max}/A$$

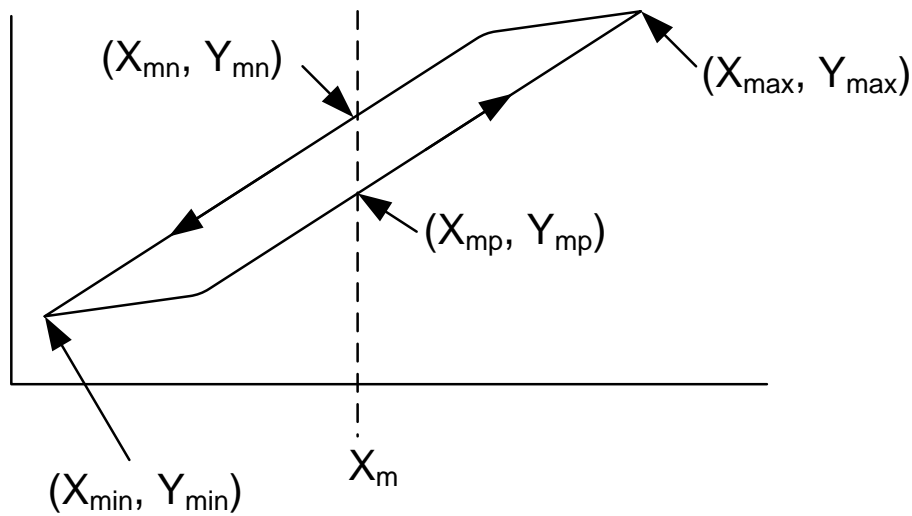
F_{max} = The maximum applied force to separate the two substrates

A = The contact area

For different samples, the adhesion test was performed for three time with the same dimension of the hydrogel samples.

3.2.7 Self-recovery test

To determine the self-recovery properties of the nanocomposite hydrogels, loading-unloading tests of these hydrogel samples were performed again on rectangular shape samples with the same dimension from the mechanical test section. In this section, the stretch ratio (λ_{\max}) was used for each sample and the samples were extended to three times of its original length and released them to their original length. Then, the samples were put in the plastic bags at room temperature to avoid water evaporation and another loading-unloading was performed again after resting the sample for 0.5 hour and 1 hour. The area enclosed between the loading and unloading curves can be defined as the dissipated energy and the recovery rate can be evaluated dividing the second cycle dissipated energy by first dissipated energy. To calculate the hysteresis recovery from the loading-unloading curves, the following formula was used.



$$\text{For midpoint location, } X_m = \left(\frac{X_{\max} - X_{\min}}{2} \right) + X_{\min}$$

$$\text{Hysteresis \%} = \left| \frac{Y_{mn} - Y_{mp}}{Y_{\max} - Y_{\min}} \right| \times 100\%$$

$$\text{Stretch ratio, } \lambda = \frac{L}{L_0}$$

L, L_0 = The length of the original and extended hydrogels

These samples were also extended to 7 times of their original length by using hand and released immediately the applied force on the samples. The samples were checked the self-recovery immediately without waiting for a long time at the ambient temperature. Then, the hydrogel samples were extended again with hand about 7 times of the initial length on the ruler and taped on two ends of the hydrogel samples with the ruler together. After that, the extended samples put at the room temperature and waited for different time (0.5 h, 1 h and 6 h) and released the hydrogel samples from extension and evaluated their recovery for lengths.

Chapter 4. Result and discussion

After testing the properties of three types of nanocomposite conductive hydrogels, the results of these hydrogels are presented including the characterisations of three types of conductive hydrogels, self-healing abilities of these hydrogels, the comparison of mechanical properties, electrical properties and self-recovery of these hydrogels between each other and before and after self-healing and adhesive properties. After presenting and comparing the various properties, these hydrogel samples was applied on most parts of human body including figures for small deformation and joints for large deformation. Then, electrochemical analyser was used to monitor the current changes while bending and stretching of the parts of human body. Finally, the discussion will be conducted based on the achieved results by comparing from the literature and the significant properties of these conductive hydrogels and some limitations of this project will be highlighted.

4.1 Characterization of nanocomposite conductive hydrogels

For the characterization of the nanocomposite hydrogels, SEM study was applied on different places of three nanocomposite hydrogels using different microscale. Figure 11 shows the morphologies differences of PAM-rGO (figure 3A), PAM-GO-rGO (Figure 11B) and PAM-GO (Figure 11C) nanocomposite hydrogels at the microscale of 20 μ m using SEM. All of these images were received by testing in the surfaces of these nanocomposite hydrogels and according to the images from the SEM, many graphene aggregations were not discovered in the surfaces of these hydrogels, which means the dispersion between PAM and graphene nanoparticles was good in these hydrogels. However, the PAM-GO hydrogels showed smooth and dense surface with very few aggregations on the surface as shown in Figure 11C while the PAM-rGO hydrogels from Figure 11A displayed a rough surface and some bubbles and few pores were found in this surface. For the PAM-GO-rGO hydrogels from Figure 11B, a relatively rough and wavy surface was observed, and more pores and bubbles were also found in the surfaces of these hydrogels.

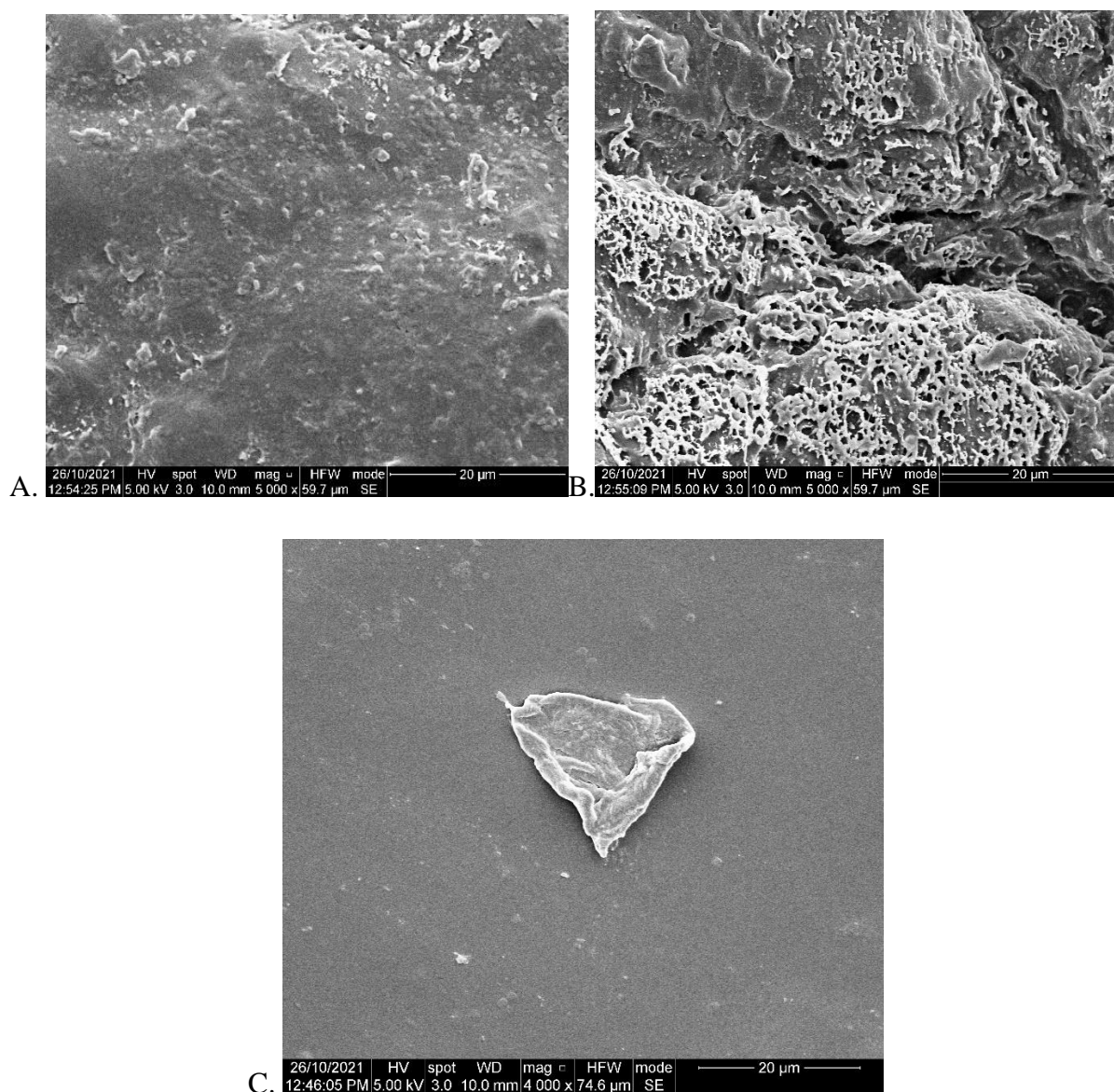


Figure 11: SEM images of graphene-based hydrogels, A. SEM image of PAM-rGO at 20 μm, B. SEM image of PAM-GO-rGO at 20 μm, C. SEM image of PAM-GO at 20 μm

4.2 Mechanical properties

The mechanical behaviour of the nanocomposite conductive hydrogels was explored with the effects of different conductive nanofillers such as GO and rGO. It was found that mechanical properties of nanocomposite hydrogels were significantly increased for PAM-rGO hydrogel when compared to PAM-GO hydrogel. Due to the different structures and specific surface area between GO and rGO, the mechanical properties of rGO-based hydrogels and GO-based hydrogels had found the differences even though the same preparation methods were used. Thus, the rGO-based nanocomposite hydrogels had shown the highest strength with 95 ± 5.2

kPa when compared with PAM-GO-rGO hydrogels and PAM-GO hydrogels. For GO-rGO-based and GO-based nanocomposite hydrogels, the strengths showed as high as 83 ± 3.6 kPa and 75.5 ± 3.3 kPa at break respectively. It was found that tensile strengths of these hydrogels with GO and rGO conductive nanofillers were higher than pure PAM hydrogels (about 37 kPa) (Chen et al., 2019). This is due to strong interactions between graphene layers and PAM which can play a role as useful strengthening in the nanocomposite conductive hydrogels to promote to high mechanical stress. The content of Fe^{3+} ions also impact on the mechanical properties of nanocomposite conductive hydrogels. A fractured hydrogel can be obtained for the hydrogels with 2% Fe^{3+} , and these hydrogels can show a quick reduction in elasticity and a growth in stiffness and brittleness. In addition, with higher amount of rGO content, the mechanical properties of the nanocomposite conductive hydrogels can be improved, and the elongation of these hydrogels can be decreased (Jing et al., 2018). Thus, with 1% of Fe^{3+} , rGO-based nanocomposite conductive hydrogels were stretched $1125 \pm 61\%$ strain at break and PAM-GO-rGO hydrogel and PAM-GO hydrogel accomplished nearly the same elongation at break with $838 \pm 46\%$ and $837 \pm 52\%$ strain respectively. Moreover, Young's modulus (E) of these conductive hydrogels were also calculated from the stress-strain curve as shown in Figure 12.

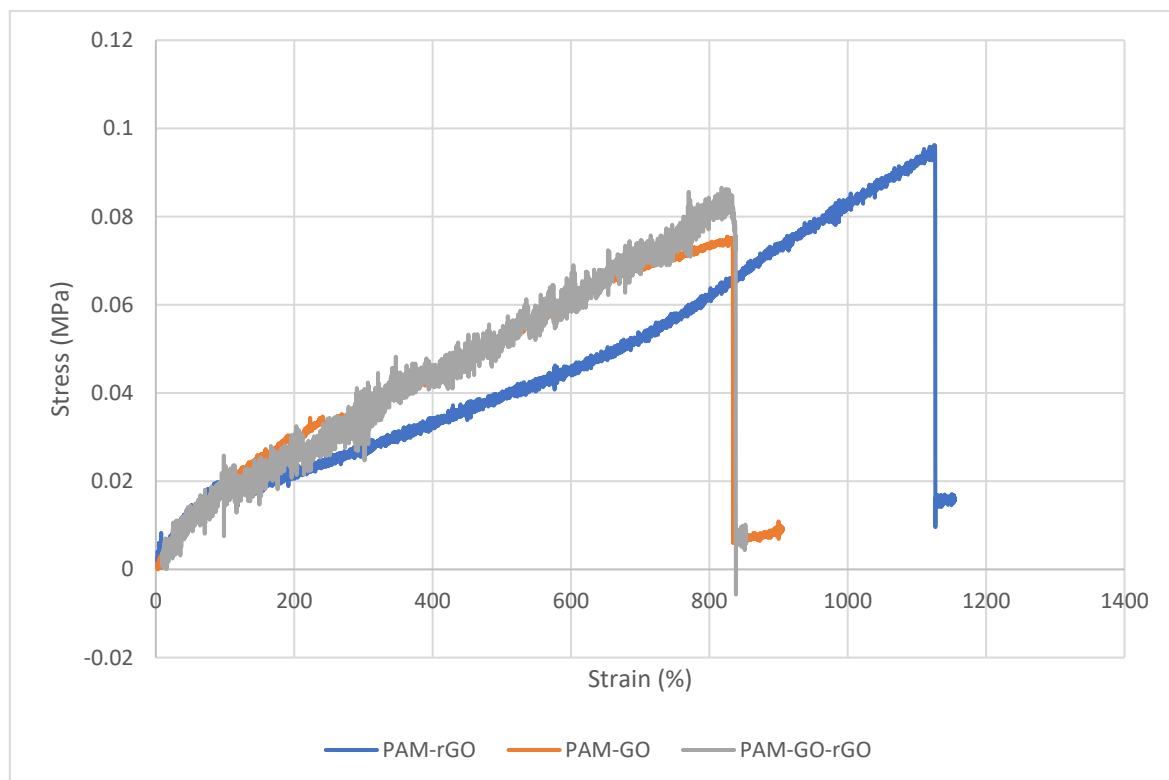


Figure 12: Stress-strain curves for mechanical behaviour of PAM-GO, PAM-rGO and PAM-GO-rGO hydrogels

| Samples | Ultimate strength (kPa) | Elongation at break | Young's modulus (Pa) |
|------------|----------------------------|---------------------|-------------------------|
| PAM-rGO | 95 ± 5.2 | 1125 ± 61% | 194 |
| PAM-GO | 75.5 ± 3.3 | 837 ± 52% | 147 |
| PAM-GO-rGO | 83 ± 3.6 | 838 ± 46% | 166 |

Table 1: Ultimate tensile strength, elongation at break and young modulus for three nanocomposite hydrogels



Figure 13: Instron tensile testing system, A. the nanocomposite hydrogels before extension and B. the nanocomposite hydrogels while extension

4.3 Electrical measurements

The electricity conductivity of the nanocomposite conductive hydrogels was studied in this project using digital multimeter (two points) and Jandel RM 3000+ (four points). The results showed that the initiation of graphene conductive nanofillers into the hydrogels increased in

both mechanical and electrical properties and also achieved the adjustable and controllable electrical conductivities. The conductivity of the original PAM hydrogels without graphene nanoparticles was almost insulating (Sun et al., 2021) and the conductivity of PAM-rGO was improved to 0.0418 S/m at the water content of 89% due to the addition of conductive nanofiller reduced graphene oxide into the PAM hydrogels. In addition, the electrical conductivity of PAM-GO was only about half of the conductivity of PAM-rGO with 0.02863 S/m at the same water content of 89%. Although graphene oxide is a type of semiconductor and do not have high conductivity, the electrical conductivity of 0.02863 S/m was achieved in the PAM-GO hydrogels due to rich water content and the content of Fe^{3+} . In the PAM-GO-rGO hydrogels, the electrical conductivity was higher the conductivity of PAM-GO hydrogels and was lower than PAM-rGO hydrogels although these PAM-GO-rGO had lower water content with the water content of 76% than both of PAM-GO and PAM-rGO hydrogels. After testing the properties of these conductive hydrogels, the light-emitting diode (LED) and the nanocomposite conductive hydrogels were connected with the circuit to know the electrical recognition of these hydrogels as shown in figure below. From the figure 9, the LED bulb was lightened as soon as the hydrogels were connected with the circuit and the LED bulb was darkened as soon as the hydrogels were disconnected with the circuit. Moreover, the strain sensitivity of the hydrogels was detected while connecting the circuit to the LED bulb with these conductive hydrogels under stretching conditions. As shown in figure, the LED bulb light power of hydrogels was lessened under the greater applied strain and when the strain was reduced into the original length of the hydrogels, it became brighter, proving the strain-sensitive behaviour. The resistance sensitivity of these hydrogels was analysed related to the strain and the results were shown in figure. For the electrical resistivity changes, the nanocomposite conductive hydrogels were extended from 20% to 200% and in all extensions, the electrical resistivity changes were recorded in the system. Then, the electrical resistivity changes were calculated with $\Delta R/R_0$ and the electrical resistivity of the hydrogel samples changed according to the tensile strain. It was found that PAM-GO hydrogel samples had the highest resistivity changes with about 260% changes at 200% strain and about 97% changes at 100% strain. For PAM-GO-rGO and PAM-rGO hydrogel samples, the resistivity changes were about 223% and 205% at 200% strain and about 70% and 40% at 100% strain, respectively. The huge resistance variations are related with the foundation for high sensitivity and high sensitivity properties are greatly demand and suitable for stain sensor devices (Cai et al., 2017). In addition, the responsive behaviour of these nanocomposite conductive hydrogels was tested depending on small and large strains as shown in the chart and it was found that these

conductive hydrogels could perform the resistivity changes from 20% to 200% deformation and thus, the sensitivity of these hydrogels worked properly for small to large deformation. The changes in the electrical resistivity under mechanical strain (piezoresistive effect) were occurred in the PAM-rGO, PAM-GO and PAM-GO-rGO nanocomposite conductive hydrogels because of two reasons. The first one was the conductivity of ion such as H^+ , Cl^- and Fe^{3+} in the hydrogel and the next one was the contact situations of the graphene-based conductive nanofillers for the electron conduction altered such as the contact part, loss of contact, and spacing changes while stretching (Jing et al., 2018). The sensitivity of these hydrogels can be quantified according to the gauge factor (G.F) which can be identified as the ratio of the relative variation of the output signal to the applied mechanical strain. In the resistive-type strain sensors, G.F was calculated by using the ratio of $\Delta R/R_0$ (the relative change of resistance) to ε (the applied strain) (Souri et al., 2020). As shown in the chart below, the resistance changes related to strain were shown with two liner regions for each hydrogel sample. For PAM-rGO hydrogel sample, the first region was 0-48% resistivity changes with 0-100% strain and the second region was 48-205% resistivity changes with 100-200% strain. For PAM-GO and PAM-GO-rGO, the first regions were 0-14.19% and 0-25.3% resistivity changes with 0-40% and 0-60% strain and the second regions were 14.19-260% and 25.3-223% resistivity changes with 40-200% and 60-200% strain, respectively. From these two liner regions, the gauge factors of each region were evaluated for three hydrogel samples and the results were listed in the table below. From the table below, the PAM-rGO conductive hydrogel sample showed the highest sensitivity in the first region with 0.5 of gauge factor when compared with the other two samples and the PAM-GO-rGO hydrogel sample showed the highest sensitivity in the second region with 1.65 of gauge factor when compared with the other two samples.

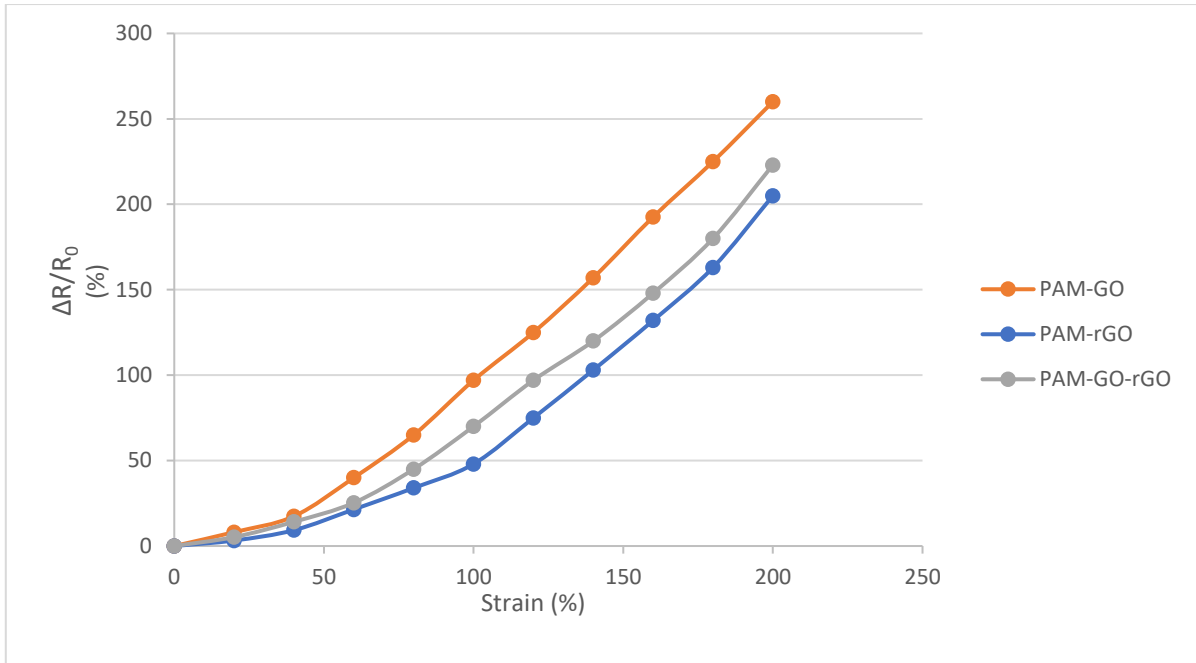


Figure 14: The resistivity changes and strain curves for the sensitivity tests of three nanocomposite hydrogels.

| Samples | Conductivity (S/m) | Water content | 1 st region GF (Strain region) | 2 nd region GF (Strain region) |
|------------|---------------------------------|---------------|---|---|
| PAM-rGO | $4.18 \pm 0.1 \times 10^{-2}$ | 89% | 0.5 (0-100%) | 1.5 (100-200%) |
| PAM-GO | $2.863 \pm 0.07 \times 10^{-2}$ | 89% | 0.35 (0-40%) | 1.54 (40-200%) |
| PAM-GO-rGO | $3.69 \pm 0.08 \times 10^{-2}$ | 76% | 0.42 (0-60%) | 1.65 (60-200%) |

Table 2: The values of electrical conductivity for three nanocomposite conductive hydrogels at different water content and gauge factor values to know sensitivity of these hydrogels for two liner regions.

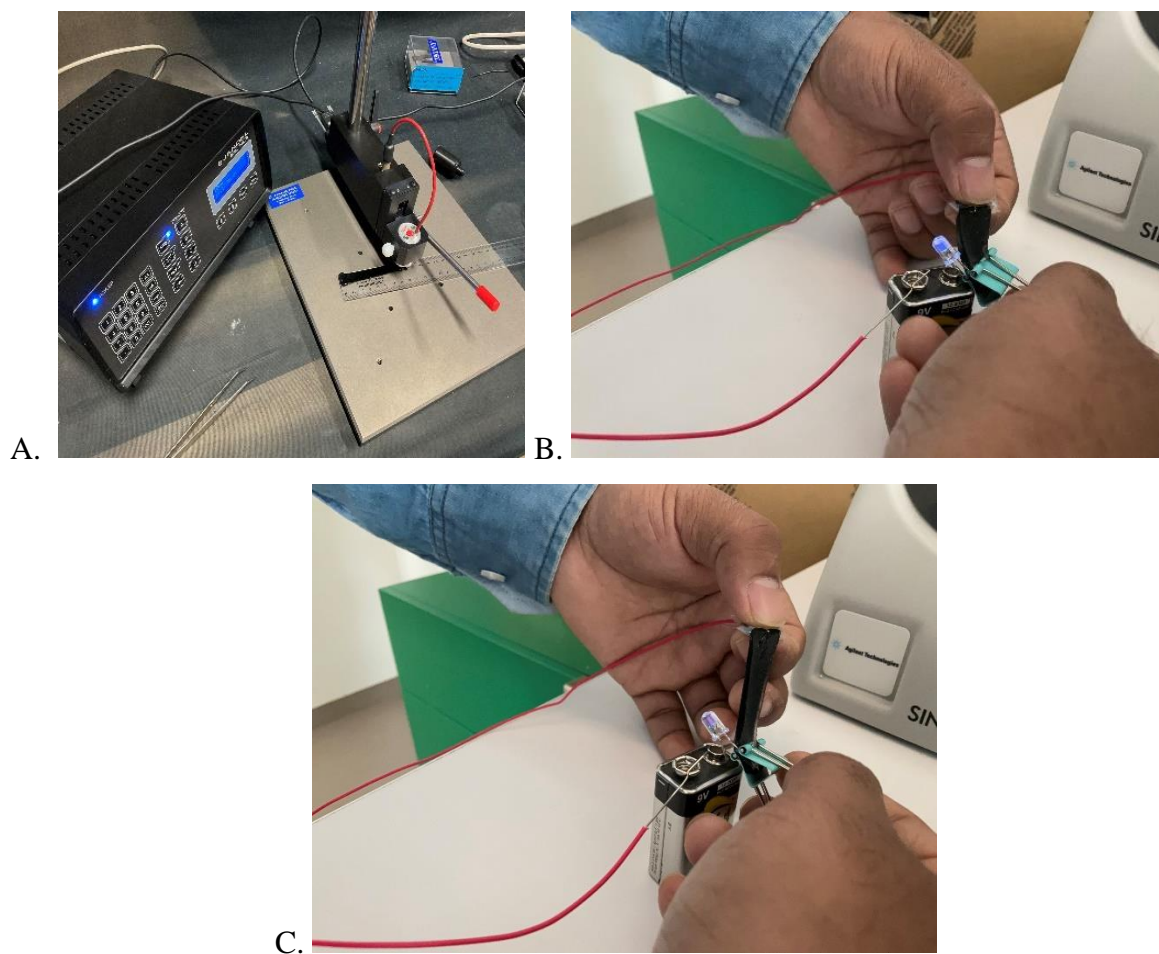


Figure 15: Testing and demonstration of electrical properties of three nanocomposite hydrogels, A. testing the electrical changes on different lengths of the samples, B. showing LED light brighter while using conductive hydrogels at normal length, C. showing the reduced brightness of LED light while using conductive hydrogels at extended length

4.4 Self-recovery properties

The self-recovery of nanocomposite conductive hydrogels was investigated by performing loading-unloading tests on the rectangular shape samples at ambient temperature without applying any external stimuli. The dimensions of these hydrogels were 25 mm length, 13 mm width and 1.3 mm thickness for PAM-GO hydrogel, 36.4 mm length, 13.5 mm width and 2 mm thickness for PAM-rGO hydrogel and 24 mm length, 12.5 mm width and 2.1 mm thickness for PAM-GO-rGO hydrogel. The recovery abilities of the nanocomposite hydrogels were assessed by using applied strain which was lower than the yielding strain (λ_{\max}). The ability of nanocomposite hydrogels to recover the original dissipated energy was evaluated by using

stretch ration of 3 and the force was set back to zero. After the first loading-unloading test, the samples were stored in the plastic bags to avoid water evaporation at the room temperature and the second and third loading-unloading tests were evaluated again after waiting for 0.5 hour and 1 hour. The area enclosed by the loading-unloading curves can be defined as the dissipated energy of the cycle and to qualify the efficiency of energy dissipated energy of the hydrogels, hysteresis measurements were needed to carry out for these hydrogels. The nanocomposite hydrogels showed the hysteresis recovery rate of 32.2 and 53.5% in dissipated energy for PAM-rGO hydrogels after 0.5 and hour at the stretch ration of 3. The hysteresis recovery rates showed 25.6 and 49.8% in dissipated energy for PAM-GO hydrogel samples and 28.3 and 51.7% in dissipated energy for PAM-GO-rGO hydrogel samples. It was observed that the recovery rate of the nanocomposite conductive hydrogels improved according to the longer resting time. When these hybrid types of hydrogels were stretched, some part of Schiff base linkages was split, and dissipated energy was found in these samples. Due to the dynamic and reversible nature of the Schiff base linkages in the hybrid hydrogels, these links can be re-formed when the external force is removed, partly recovering the initial mechanical properties. Schiff base linkages could be more reformed while resting time was longer, which could result in higher dissipated energy recovery rate of these hybrid hydrogels. Moreover, any external stimuli were not required to re-established quickly these reversible Schiff base linkages at room temperature when these linkages were broken and these linkages lead to the self-healing of the inner injury of hydrogel network (Huang et al., 2019).

Then, each sample was extended to the maximum length before breaking by hand at ambient temperature as displayed in figure 16 and released the sample. In the first test, the PAM-rGO hydrogel was extended to 250mm length and released immediately to 37 mm from 36.4 mm initial length and in PAM-GO and PAM-GO-rGO hydrogels, the samples were extended to 180 mm and 145 mm length and released immediately to 27 mm from 25 mm initial length and 25 mm length from 24 mm initial length, respectively. In the second test, the hydrogel samples were extended to their maximum length by hand and the end of these hydrogels were taped together with the ruler by waiting for 1 hour and 3 hours. After 1 hour, the PAM-rGO hydrogel was released and achieved 37.6 mm and in PAM-GO and PAM-GO-rGO hydrogels, the samples were released to 28.1 mm and 26 mm length, respectively. After 3 hours, the lengths were 38 mm for PAM-rGO sample, 28.9 mm for PAM-GO sample and 27.1 mm for PAM-GO-rGO. It was also found that they can be more recovered to their initial length with longer

resting time and interestingly, all samples were recovered to their original lengths within 2.5 hours at the room temperature.

| Samples | Recovery rate (0.5 hr) | Recovery rate (1 hr) | Length changes | Length after 1hr holding | Length after 3 hr holding |
|------------|------------------------|----------------------|----------------|--------------------------|---------------------------|
| PAM-rGO | 32.2% | 53.5% | 1.64% | 3.29% | 4.39% |
| PAM-GO | 25.6% | 49.8% | 8% | 12.4% | 15.6% |
| PAM-GO-rGO | 28.3% | 51.7% | 4.16% | 8.33% | 12.92% |

Table 3: The recovery rate of three nanocomposite hydrogels according to dissipated energy after 0.5 and 1 hour and the length changes percent after extending the samples to maximum length and releasing to normal state.

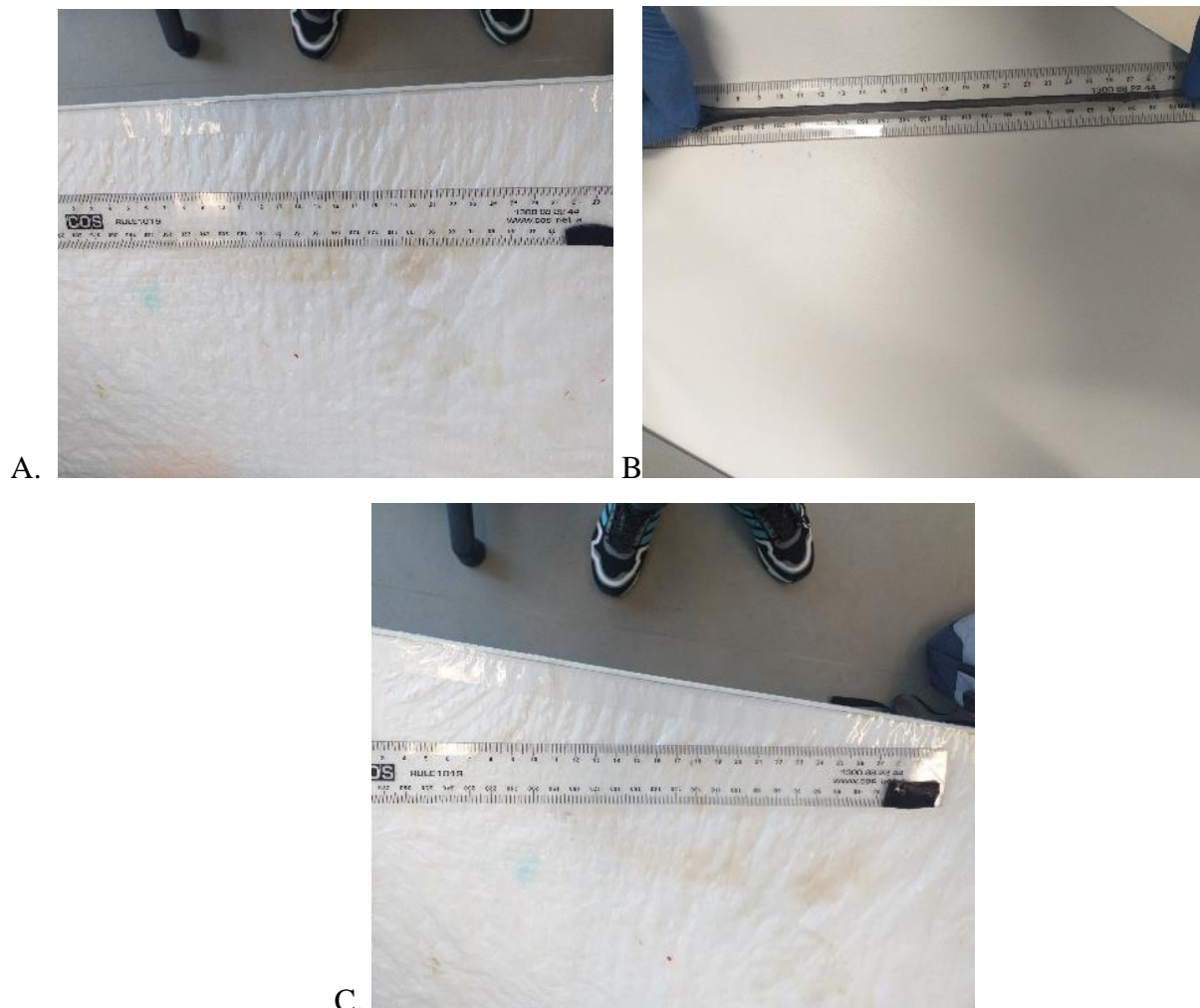


Figure 16: The extension of the samples into 7 times of original length and releasing nearly to its initial length, A. Before extension, B. while extension, C. after extension

4.5 Self-healing properties

To examine the self-healing properties of the nanocomposite conductive hydrogels, these hydrogel samples were cut into two pieces and contact again in the fridge for 2 days. Then, the tensile properties, electrical properties and self-recovery properties were tested again and compared the results before and after self-healing with the same dimensions of the samples. After self-healing, the PAM-rGO hydrogel samples showed the highest ultimate stress in the same way as before self-healing with 84 ± 6.3 kPa and in PAM-GO-rGO and PAM-GO hydrogels, the ultimate strength showed 80.7 ± 5.8 kPa and 66.78 ± 5.5 kPa, respectively. In addition, the strains of these hydrogels were dropped from about 1125% to 940% for PAM-rGO, from about 838% to 797% for PAM-GO-rGO and from about 837% to 749% for PAM-GO hydrogels. The tensile strength of these hydrogels after self-healing were about 84-97% of original hydrogels with 97.22% for PAM-GO-rGO, 88.45% for PAM-GO and 88.4% for PAM-rGO. Moreover, the tensile strain of PAM-GO-rGO hydrogels after self-healing were about 95.11% of original hydrogels, 89.48% for PAM-GO and 83.55 for PAM-rGO. This suggests that these nanocomposite hydrogels had a good self-healing quality, and this quality was achieved due to the content of PDA in these nanocomposite hydrogels. Firstly, the interactions were caused between free catechol groups of the PDA chains and amino groups of PAM by linking the PDA chains within PAM network. Then, the reversible noncovalent bonds such as hydrogen bonding and π - π stacking could be generated at the injured interface due to phenolic hydroxyl groups. These reversible bonds caused the self-healing properties on the PAM hydrogels after damage without any external stimuli. As some of the chemical crosslinking points could be broken and unrecovered, the mechanical properties of these hydrogels dropped (Huang et al., 2020).

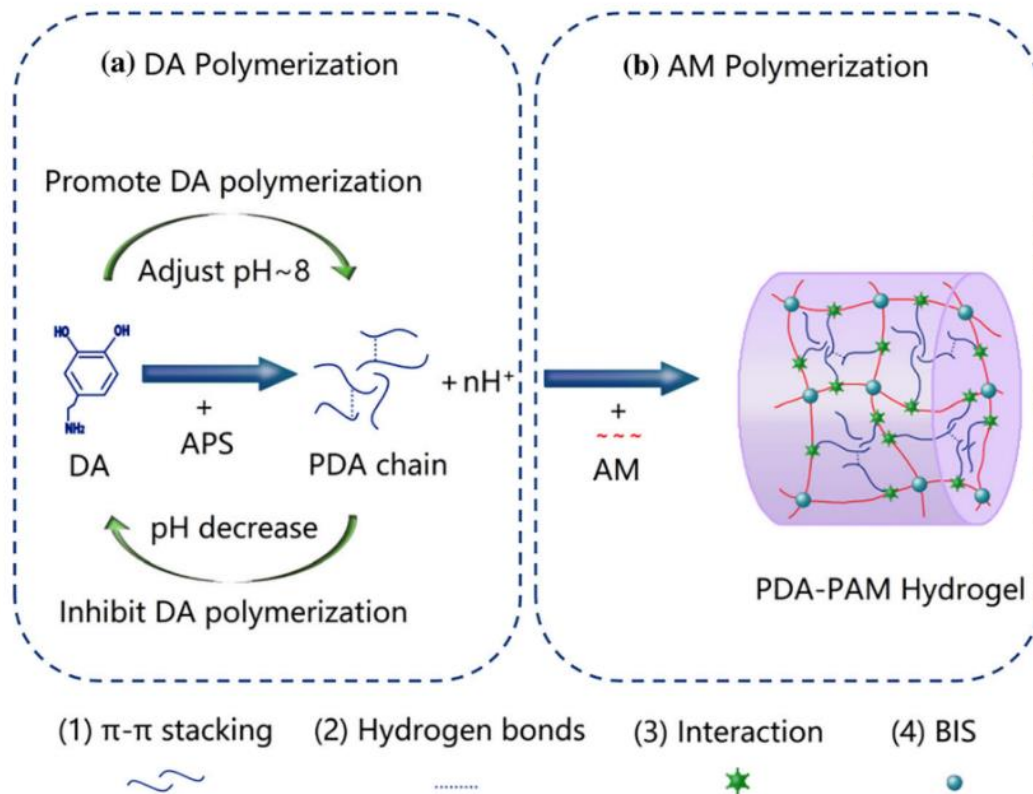


Figure 17: The structure of PAM with PDA and the formation of reversible bonds inside the hydrogels.

The electrical behaviour of the healed nanocomposite hydrogels was also investigated after self-healing of the samples from two pieces. Firstly, the electrical conductivity of the healed hydrogels was tested using digital multimeter (two points) and Jandel RM 3000+ (four points) and showed $3.99 \pm 0.08 \times 10^{-2}$ S/m for PAM-rGO with the highest conductivity among three samples at the water content of 87%. At the same water content, PAM-GO hydrogels achieved $2.44 \pm 0.12 \times 10^{-2}$ S/m and PAM-GO-rGO showed the conductivity of $3.48 \pm 0.1 \times 10^{-2}$ S/m at the water content of 73%. In the PAM-rGO hydrogels, the conductivity was reduced from about 4.18×10^{-2} to 3.99×10^{-2} S/m after self-healing and the healing rate was about 95.46% in this hydrogel. In addition, the conductivity of PAM-GO and PAM-GO-rGO hydrogels also reduced from 2.86×10^{-2} to 2.44×10^{-2} S/m and from 3.69×10^{-2} to 3.48×10^{-2} and showed good healing rate with 85.31% and 94.3% respectively. According to the healing rate with 85-95% for conductivity of these hydrogels, it recovered to nearly its original conductivity and also indicated that the conductivity of these hydrogels was impacted in the broken area.

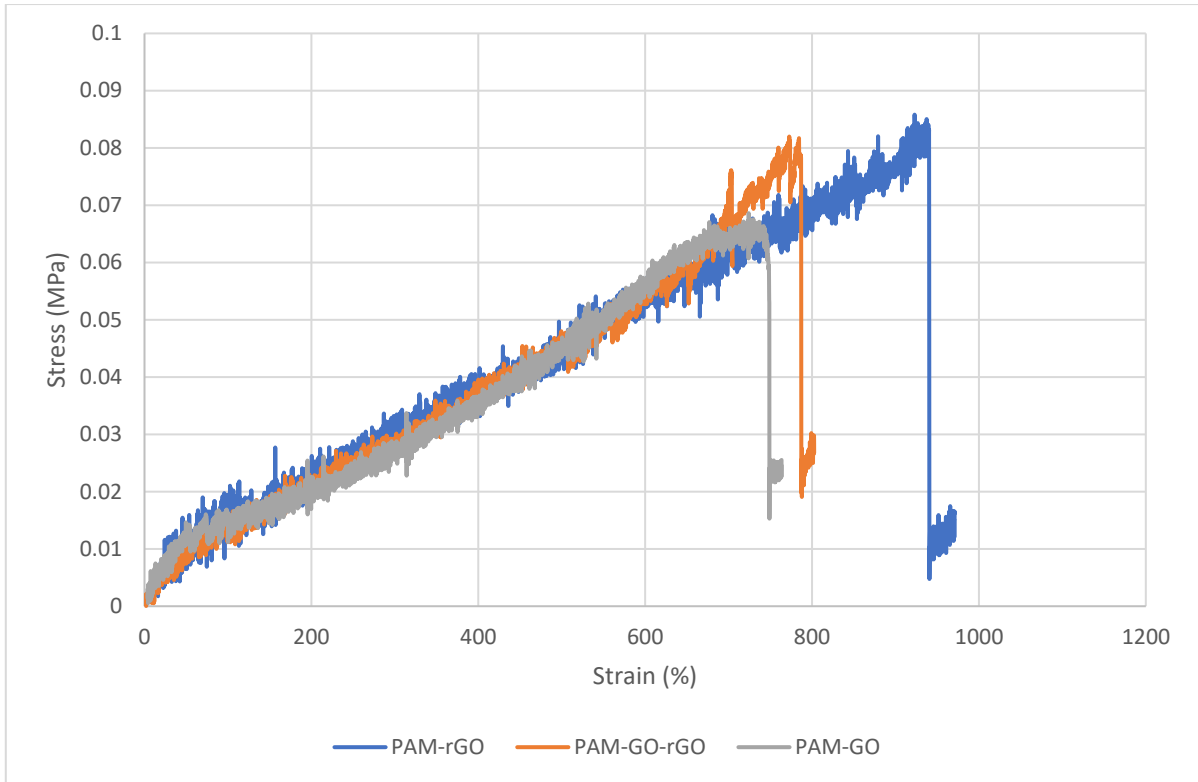


Figure 18: The stress-strain curves for the mechanical behaviour of three nanocomposite hydrogels after self-healing

| Samples | Tensile strength before / after self-healing (kPa) | Elongation before and after self-healing | Young's Modulus before and after self-healing (Pa) |
|------------|--|--|--|
| PAM-rGO | $95 \pm 5.2 / - 84 \pm 6.3$ | 1125% / - 940% | 194 / - 177 |
| PAM-GO | $75.5 \pm 3.3 / - 66.78 \pm 5.5$ | 837% / - 749% | 171 / - 167 |
| PAM-GO-rGO | $83 \pm 3.6 / - 80.7 \pm 5.8$ | 838% / - 797% | 166 / - 152 |

Table 4: Tensile strength values, elongation values at break and young modulus values before and after self-healing

| Samples | Strength recovery | Strain recovery | Young's modulus recovery |
|---------|-------------------|-----------------|--------------------------|
| PAM-rGO | 88.42 % | 83.56 % | 91.24 % |

| | | | |
|------------|---------|---------|---------|
| PAM-GO | 88.45 % | 89.48 % | 95.9% |
| PAM-GO-rGO | 97.23 % | 95.11 % | 91.57 % |

Table 5: The recovery rate of tensile strength, strain, and Young modulus after self-healing

| Samples | Conductivity before / after self-healing ($\times 10^{-2}$ S/m) | Water content (%) | Conductivity recovery |
|------------|--|-------------------|-----------------------|
| PAM-rGO | 4.18 \pm 0.1 / 3.99 \pm 0.08 | 89 / 87 | 95% |
| PAM-GO | 2.863 \pm 0.07 / 2.44 \pm 0.12 | 89 / 87 | 85.22% |
| PAM-GO-rGO | 3.69 \pm 0.08 / 3.48 \pm 0.1 | 76 / 73 | 94.3% |

Table 6: The electrical conductivity of three nanocomposite hydrogels before and after self-healing at different water content, the recovery rate of electrical conductivity after self-healing

4.6 Adhesive properties

Originally, the hydrogel could show excellent adhesive properties to most surfaces such as skin, glassware, plastic and metal due to their abundant catechol groups (Zhang et al., 2021). By interacting with amine or thiol groups, the free catechol groups from the PDA caused cation- π or π - π interactions with other contact surfaces and the adhesive properties were occurred due to these interactions. If the two uncut surfaces were contacted together, they could attach to each other and can be split up by pulling as many active catechol from the freshly cut surfaces caused strong self-healing and the catechol groups from the uncut surfaces caused adhesion (Han et al., 2017). Thus, the nanocomposite hydrogels also achieved good adhesive properties and they adhered to most surfaces including skin, plastic, glass and metal as shown in figure 18. The adhesive properties of these hydrogels were also performed on human skin while bending and stretching as shown in figure 12 and showed that these hydrogels could keep sufficient adhesion during deformation without peeling off from the fingers and can be simply peeled off from the fingers without any remainders or damage. Moreover, these hydrogels could get back to its original state after bending and stretching and demonstrated the excellent skin attraction of the hydrogels. Thus, these remarkable adhesive properties of hydrogels would provide them with potential opportunities to use in the field of biomedical applications. In order to assess the adhesive abilities of these nanocomposite hydrogels, the adhesive forces were calculated depending on the weigh they carried without peeling off on various substrates. The

adhesive strength is greatly dependent on surface energy which means the higher the surface energy, it is easier the adhesives stick to these surfaces (Zhang et al., 2021). Thus, some kind of substrates were used in this project to know with different energies and different adhesive forces. It showed the glass have highest adhesive properties when compared with other steel and plastic materials, following the order plastic < steel < glass. In glass, the adhesive strength of PAM-GO hydrogels was the highest with 3923 ± 12 Pa and the other PAM-GO-rGO and PAM-rGO hydrogels were 3652 ± 13 Pa and 3289 ± 10 Pa, respectively. In stainless steel, the adhesive strength showed 2825 ± 11 Pa for PAM-GO hydrogel, 2693 ± 13 Pa for PAM-GO-rGO and 2558 ± 12 Pa for PAM-rGO. Finally, for plastic materials, the adhesive strengths were 2621 ± 10 Pa for PAM-GO, 2562 ± 12 Pa for PAM-GO-rGO and 2446 ± 12 Pa for PAM-rGO.

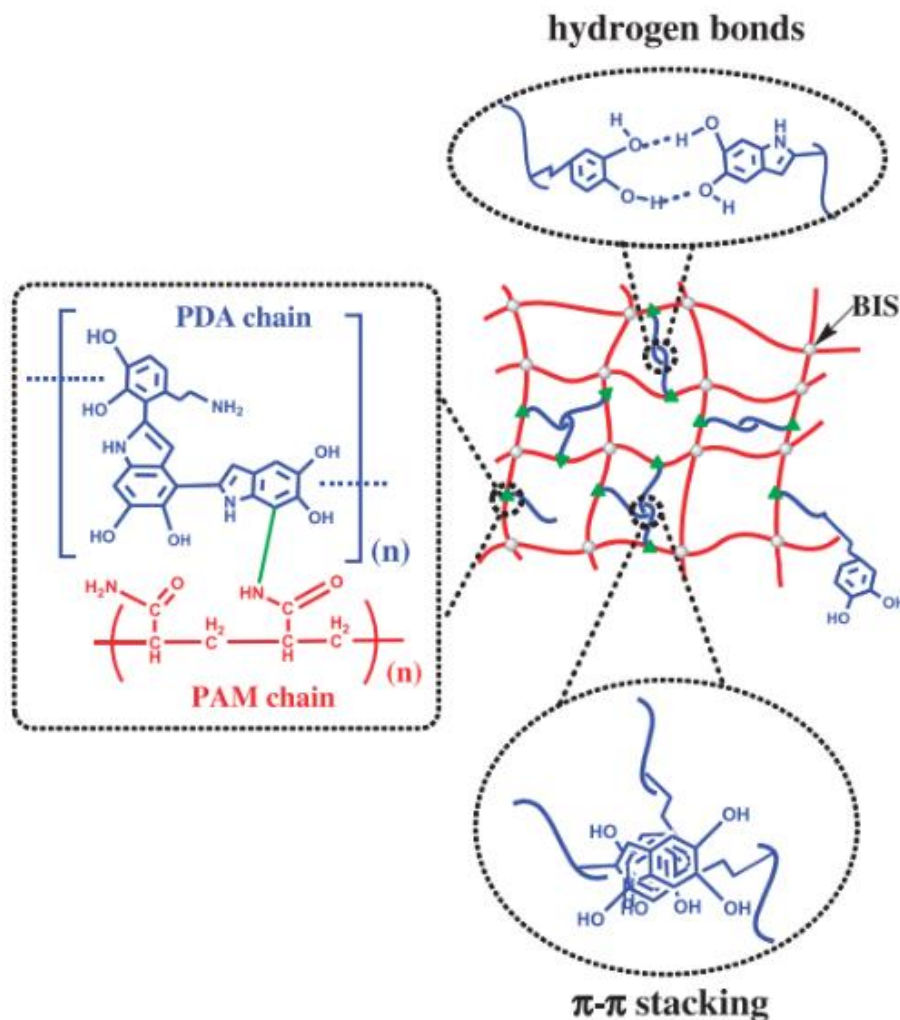


Figure 19: The interactions between free catechol groups which caused adhesion and the amino groups of PAM at green triangles and the reversible bonds formed between the catechol groups of the PDA chains

| Samples | Adhesive strength on glass (Pa) | Adhesive strength on steel (Pa) | Adhesive strength on plastic (Pa) |
|------------|---------------------------------|---------------------------------|-----------------------------------|
| PAM-rGO | 3289 ± 10 | 2558 ± 12 | 2446 ± 12 |
| PAM-GO | 3923 ± 12 | 2825 ± 11 | 2621 ± 10 |
| PAM-GO-rGO | 3652 ± 13.5 | 2693 ± 13 | 2562 ± 12 |

Table 7: The various adhesive strength of three nanocomposite hydrogels on different substrates such as glass, steel and plastic



Figure 20: The demonstration of the adhesive properties on different substrates including skin, glassware, steel, and plastic

Chapter 5 Conclusion

In summary, three types of nanocomposite conductive hydrogels were successfully fabricated using graphene-based conductive nanofillers. The properties of these three nanocomposite conductive hydrogels were analysed and the effects and differences of these hydrogels had compared each other. It was observed that the mechanical and electrical properties of the hydrogels were increased by adding graphene-based conductive nanofillers into the pure PAM hydrogels. Among fabricated three samples, rGO-based nanocomposite hydrogels were more effective than the other two nanocomposite hydrogels fabricated by using GO and GO-rGO combination, in terms of improving the strength and elongation of the hydrogels. Although the higher elongation values were achieved in all nanocomposite hydrogels, the young modulus (E) of these hydrogels should be higher than the current values. It was also found that in all graphene-based nanocomposite hydrogels, good conductivity was achieved although the conductivity properties of pure PAM hydrogels were almost insulating. Among three conductive hydrogels, it was discovered that rGO-based hydrogels had higher conductivity than the other two hydrogels. It was clear that good conductivity was achieved in all nanocomposite hydrogels due to graphene nanoparticles, high water content and the content of Fe^{3+} . The content of Fe^{3+} in the hydrogels partially helped to improve their conductivity and also helped to self-heal for these hydrogels. Without Fe^{3+} , the self-healing behaviour was not found in the hydrogels and thus, the relocation of Fe^{3+} played an important role to achieve self-healing behaviour in the hydrogels. Moreover, these nanocomposite hydrogels self-healed 88-93% of original tensile strength, 83-95% of original strain and 85-95% of electrical conductivity. The sensitivity properties of the nanocomposite hydrogels were tested depending on the resistivity changes ratio according to stain and the gauge factors were evaluated from resistivity changes-strain curve. From the curve, two liner regions were found in each sample and 0.35-0.5 G.F was shown in the first region and 1.5-1.65 G.F was shown in the second region for these hydrogels, respectively. Moreover, around 50% in dissipated energy of self-recovery was found in these hydrogels after resting for 1 hour and in longer resting time, more than 50% recovery rate can be achieved in these hydrogels. In addition, good adhesive properties were found in these nanocomposite hydrogels on most substrates, including skin, glass, steel and plastics. After preparing the graphene-based hydrogels and evaluating their most important properties, these hydrogels showed good mechanical, electrical, self-recovery, self-healing and adhesive properties and in all properties, these hydrogels were better than pure PAM hydrogels. Thus, these hydrogels can be used in wider applications in most fields,

including biomedical applications and the combination of mechanical, electrical, self-healing, self-recovery and adhesive properties makes these nanocomposite hydrogels a promising material for some applications such as strain sensors, soft robotic materials and human skins.

Chapter 6 Future work

In this thesis, the graphene-based nanocomposite hydrogels were fabricated, analysed and improved their various properties compared to conventional hydrogels and also focused to use these hydrogels on wider range of applications including biosensors. In this thesis, only graphene-based nanoflakes and FeCl₃ were added into the conventional hydrogels and the enhancement was found in various properties including electrical properties although traditional hydrogels were almost insulating. However, in the future, hyper-branched polymers and carbon nanotubes and graphene oxide combination can be provided higher mechanical and electrical properties of nanocomposite hydrogels. At present, two types of difficulties were faced during the preparation of nanocomposite conductive hydrogels. Because of the rich water content in the polymer network, the hydrogels can show weak mechanical behavior and thus, hyper-branched polymers are ideal candidate as the toughening agents for the hydrogels to achieve supramolecular connections with hydrogels networks. For example, Xing et al., developed a nanocomposite hydrogel with enriched hyper-branched polymers and these types of hydrogels showed higher strength with 140 kPa, young modulus with 120 kPa in these hydrogels due to the presence of many hydroxyl groups on the hyper-branched polymers structure which can develop hydrogen bonding with the carboxylic groups (Xing et al., 2021). Moreover, due to low solubility of reduced graphene oxide, it was difficult to achieve the homogeneity between reduced graphene oxide and polyacrylamide monomer while adding higher percent of reduced graphene oxide in the polyacrylamide monomer. Therefore, introducing CNTs and GO combination in the polyacrylamide would increase the electrical conductivity and sensitivity of nanocomposite hydrogels. For example, Zhang et al., fabricated carbon nanotube and graphene combination-based hydrogels and these hydrogels showed higher conductivity with the resistivity from 3 to 0.79 Ω (Zhang et al., 2019). As two types of conductive nanofillers are linked together while large deformation and mechanical properties are strong due to enriched hyper-branched polymers, carbon nanotube and graphene oxide combination-based hydrogels with enriched hyper-branched polymers would be huge possibilities to use in the biomedical applications such as biosensors in the future.

References

- Adhikari, B., Biswas, A., & Banerjee, A. (2012). Graphene oxide-based hydrogels to make metal nanoparticle-containing reduced graphene oxide-based functional hybrid hydrogels. *ACS Applied Materials & Interfaces*, 4(10), 5472-5482.
- Biondi, M., Borzacchiello, A., Mayol, L., & Ambrosio, L. (2015). Nanoparticle-integrated hydrogels as multifunctional composite materials for biomedical applications. *Gels*, 1(2), 162-178.
- Cai, G., Wang, J., Qian, K., Chen, J., Li, S., & Lee, P. S. (2017). Extremely stretchable strain sensors based on conductive self-healing dynamic cross-links hydrogels for human-motion detection. *Advanced Science*, 4(2), 1600190.
- Chen, J., Peng, Q., Thundat, T., & Zeng, H. (2019). Stretchable, injectable, and self-healing conductive hydrogel enabled by multiple hydrogen bonding toward wearable electronics. *Chemistry of Materials*, 31(12), 4553-4563.
- Chen, Y., Zheng, K., Niu, L., Zhang, Y., Liu, Y., Wang, C., & Chu, F. (2019). Highly mechanical properties nanocomposite hydrogels with biorenewable lignin nanoparticles. *International Journal of Biological Macromolecules*, 128, 414-420.
- Gan, D., Han, L., Wang, M., Xing, W., Xu, T., Zhang, H., ... & Lu, X. (2018). Conductive and tough hydrogels based on biopolymer molecular templates for controlling in situ formation of polypyrrole nanorods. *ACS Applied Materials & Interfaces*, 10(42), 36218-36228.
- Guo, B., Ma, Z., Pan, L., & Shi, Y. (2019). Properties of conductive polymer hydrogels and their application in sensors. *Journal of Polymer Science Part B: Polymer Physics*, 57(23), 1606-1621.
- Han, L., Yan, L., Wang, K., Fang, L., Zhang, H., Tang, Y., ... & Lu, X. (2017). Tough, self-healable and tissue-adhesive hydrogel with tunable multifunctionality. *NPG Asia Materials*, 9(4), e372-e372.
- Huang, J., Zhang, W., Li, H., Yu, X., Ding, S., & Wu, C. (2020). An autonomous self-healing hydrogel with high polydopamine content for improved tensile strength. *Journal of Materials Science*, 55(36), 17255-17265.

- Huang, W., Wang, Y., McMullen, L. M., McDermott, M. T., Deng, H., Du, Y., ... & Zhang, L. (2019). Stretchable, tough, self-recoverable, and cytocompatible chitosan/cellulose nanocrystals/polyacrylamide hybrid hydrogels. *Carbohydrate Polymers*, 222, 114977.
- Jing, X., Mi, H. Y., Peng, X. F., & Turng, L. S. (2018). Biocompatible, self-healing, highly stretchable polyacrylic acid/reduced graphene oxide nanocomposite hydrogel sensors via mussel-inspired chemistry. *Carbon*, 136, 63-72.
- Jo, H., Sim, M., Kim, S., Yang, S., Yoo, Y., Park, J. H., ... & Lee, J. Y. (2017). Electrically conductive graphene/polyacrylamide hydrogels produced by mild chemical reduction for enhanced myoblast growth and differentiation. *Acta Biomaterialia*, 48, 100-109.
- Johnson, D. W., Dobson, B. P., & Coleman, K. S. (2015). A manufacturing perspective on graphene dispersions. *Current Opinion in Colloid & Interface Science*, 20(5-6), 367-382.
- Ma, J., Liu, J., Zhu, W., & Qin, W. (2018). Solubility study on the surfactants functionalized reduced graphene oxide. *Colloids and Surfaces A: Physicochemical and Engineering Aspects*, 538, 79-85.
- Matos-Perez, C. R., White, J. D., & Wilker, J. J. (2012). Polymer composition and substrate influences on the adhesive bonding of a biomimetic, cross-linking polymer. *Journal of the American Chemical Society*, 134(22), 9498-9505.
- Mihajlovic, M., Mihajlovic, M., Dankers, P. Y., Masereeuw, R., & Sijbesma, R. P. (2019). Carbon nanotube reinforced supramolecular hydrogels for bioapplications. *Macromolecular Bioscience*, 19(1), 1800173.
- Li, Z., Wei, J., Ren, J., Wu, X., Wang, L., Pan, D., & Wu, M. (2019). Hierarchical construction of high-performance all-carbon flexible fiber supercapacitors with graphene hydrogel and nitrogen-doped graphene quantum dots. *Carbon*, 154, 410-419.
- Liu, Y., Liu, J., Yang, H., Liu, K., Miao, R., Peng, H., & Fang, Y. (2018). Dynamic covalent bond-based hydrogels with superior compressive strength, exceptional slice-resistance and self-healing properties. *Soft Matter*, 14(39), 7950-7953.
- Liu, S., Qiu, Y., Yu, W., & Zhang, H. (2020). Highly stretchable and self-healing strain sensor based on gellan gum hybrid hydrogel for human motion monitoring. *ACS Applied Polymer Materials*, 2(3), 1325-1334.

Obodo, R. M., Ahmad, I., & Ezema, F. I. (2019). Introductory chapter: graphene and its applications. In *Graphene and Its Derivatives-Synthesis and Applications*. Intechopen.

Ray, S. C. (2015). Application and uses of graphene oxide and reduced graphene oxide. *Applications of Graphene and Graphene-Oxide Based Nanomaterials*, 1.

Shukla, S., & Shukla, A. (2018). Tunable antibiotic delivery from gellan hydrogels. *Journal of Materials Chemistry B*, 6(40), 6444-6458.

Smith, A. T., LaChance, A. M., Zeng, S., Liu, B., & Sun, L. (2019). Synthesis, properties, and applications of graphene oxide/reduced graphene oxide and their nanocomposites. *Nano Materials Science*, 1(1), 31-47.

Souri, H., Banerjee, H., Jusufi, A., Radacsi, N., Stokes, A. A., Park, I., ... & Amjadi, M. (2020). Wearable and stretchable strain sensors: materials, sensing mechanisms, and applications. *Advanced Intelligent Systems*, 2(8), 2000039.

Sun, F., Huang, X., Wang, X., Liu, H., Wu, Y., Du, F., & Zhang, Y. (2021). Highly transparent, Adhesive, stretchable and conductive PEDOT: PSS/polyacrylamide hydrogels for flexible strain sensors. *Colloids and Surfaces A: Physicochemical and Engineering Aspects*, 126897.

Tai, Z., Yang, J., Qi, Y., Yan, X., & Xue, Q. (2013). Synthesis of a graphene oxide–polyacrylic acid nanocomposite hydrogel and its swelling and electroresponsive properties. *RSC Advances*, 3(31), 12751-12757.

Tang, L., Wu, S., Qu, J., Gong, L., & Tang, J. (2020). A review of conductive hydrogel used in flexible strain sensor. *Materials*, 13(18), 3947.

Vashist, A., Kaushik, A., Vashist, A., Sagar, V., Ghosal, A., Gupta, Y. K., ... & Nair, M. (2018). Advances in carbon nanotubes–hydrogel hybrids in nanomedicine for therapeutics. *Advanced Healthcare Materials*, 7(9), 1701213.

Wahid, F., Zhao, X. J., Jia, S. R., Bai, H., & Zhong, C. (2020). Nanocomposite hydrogels as multifunctional systems for biomedical applications: Current state and perspectives. *Composites Part B: Engineering*, 108208.

Walker, B. W., Lara, R. P., Mogadam, E., Yu, C. H., Kimball, W., & Annabi, N. (2019). Rational design of microfabricated electroconductive hydrogels for biomedical applications. *Progress in Polymer Science*, 92, 135-157.

Xing, W., Ghahfarokhi, A. J., Xie, C., Naghibi, S., Campbell, J. A., & Tang, Y. (2021). Mechanical properties of a supramolecular nanocomposite hydrogel containing hydroxyl groups enriched hyper-branched polymers. *Polymers*, 13(5), 805.

Xu, J., Tsai, Y. L., & Hsu, S. H. (2020). Design strategies of conductive hydrogel for biomedical applications. *Molecules*, 25(22), 5296.

Yang, C., Liu, Z., Chen, C., Shi, K., Zhang, L., Ju, X. J., ... & Chu, L. Y. (2017). Reduced graphene oxide-containing smart hydrogels with excellent electro-response and mechanical properties for soft actuators. *ACS applied materials & interfaces*, 9(18), 15758-15767.

Yang, T. (2012). Mechanical and swelling properties of hydrogels (Doctoral dissertation, KTH Royal Institute of Technology).

Yang, Y., Wang, X., Yang, F., Shen, H., & Wu, D. (2016). A universal soaking strategy to convert composite hydrogels into extremely tough and rapidly recoverable double-network hydrogels. *Advanced Materials*, 28(33), 7178-7184.

Yu, Y., De Andrade, L. C. X., Fang, L., Ma, J., Zhang, W., & Tang, Y. (2015). Graphene oxide and hyperbranched polymer-toughened hydrogels with improved absorption properties and durability. *Journal of Materials Science*, 50(9), 3457-3466.

Yun, J., Im, J. S., Lee, Y. S., Yoo, S. J., & Kim, H. I. (2011). Sustained release behavior of pH-responsive poly (vinyl alcohol)/poly (acrylic acid) hydrogels containing activated carbon fibers. *Journal of Applied Polymer Science*, 120(2), 1050-1056.

Zhang, H., Ji, X., Liu, N., & Zhao, Q. (2019). Synergy effect of carbon nanotube and graphene hydrogel on highly efficient quantum dot sensitized solar cells. *Electrochimica Acta*, 327, 134937.

Zhang, X., Chen, J., He, J., Bai, Y., & Zeng, H. (2021). Mussel-inspired adhesive and conductive hydrogel with tunable mechanical properties for wearable strain sensors. *Journal of Colloid and Interface Science*, 585, 420-432.

Zhao, H., Liu, M., Zhang, Y., Yin, J., & Pei, R. (2020). Nanocomposite hydrogels for tissue engineering applications. *Nanoscale*, 12(28), 14976-14995.

Zhong, M., Liu, Y. T., Liu, X. Y., Shi, F. K., Zhang, L. Q., Zhu, M. F., & Xie, X. M. (2016). Dually cross-linked single network poly (acrylic acid) hydrogels with superior mechanical properties and water absorbency. *Soft Matter*, 12(24), 5420-5428.

Zhou, L., Fan, L., Yi, X., Zhou, Z., Liu, C., Fu, R., ... & Ning, C. (2018). Soft conducting polymer hydrogels cross-linked and doped by tannic acid for spinal cord injury repair. *ACS Nano*, 12(11), 10957-10967.

Zhu, L., Lu, Y., Wang, Y., Zhang, L., & Wang, W. (2012). Preparation and characterization of dopamine-decorated hydrophilic carbon black. *Applied Surface Science*, 258(14), 5387-5393.